4-2016

High-Purity Oxygen Production Using Mixed Ionic-Electronic Conducting Sorbents

Chandler C. Dorris
University of Pennsylvania, chdorris@seas.upenn.edu

Eric Lu
University of Pennsylvania, ericlu@sas.upenn.edu

Sangjae Park
University of Pennsylvania, sangjaep@seas.upenn.edu

Fabian H. Toro
University of Pennsylvania, fabiant@seas.upenn.edu

High-Purity Oxygen Production Using Mixed Ionic-Electronic Conducting Sorbents

Abstract
This project evaluates the potential of new, mixed ionic-electronic conducting (MIEC) materials in the production of high-purity oxygen. Analyzing today's proven MIEC properties, we design an optimized process for the production of oxygen at 30 metric tons/day. This report includes a detailed model of MIECs performance in a vacuum swing adsorption system. A sensitivity analysis is also included, which is used to optimize the operating conditions and other design variables. Based on an oxygen selling price of $40 per ton, the realized process would operate at a loss in today's economy. The total capital investment of the plant is $1.1 million and the expected NPV of the project is a loss of $87,000. The estimated IRR of the project is -28.08% and the 3-year ROI is -7.4%. Breakeven would occur at a price of $56.70.

Disciplines
Biochemical and Biomolecular Engineering | Chemical Engineering | Engineering

High-Purity Oxygen Production Using Mixed Ionic-Electronic Conducting Sorbents

Chandler Dorris
Sangjae Park
Eric Lu
Fabian Toro

April 14, 2016

Faculty Advisor
Dr. Talid Sinno, University of Pennsylvania

Industry Consultant
Dr. Matthew Targett, LP Amina

Department of Chemical and Biomolecular Engineering School of Engineering and Applied Science
University of Pennsylvania

Abstract

This project evaluates the potential of new, mixed ionic-electronic conducting (MIEC) materials in the production of high-purity oxygen. Analyzing today's proven MIEC properties, we design an optimized process for the production of oxygen at 30 metric tons/day. This report includes a detailed model of MIECs performance in a vacuum swing adsorption system. A sensitivity analysis is also included, which is used to optimize the operating conditions and other design variables. Based on an oxygen selling price of $40 per ton, the realized process would operate at a loss in today's economy. The total capital investment of the plant is $1.1 million and the expected NPV of the project is a loss of $87,000. The estimated IRR of the project is -28.08% and the 3-year ROI is -7.4%. Breakeven would occur at a price of $56.70.

Table of Contents

To the Department of Chemical and Biomolecular Engineering:

We respectfully submit this report in partial fulfillment of the requirements for the Bachelor of Science Engineering Degree in chemical engineering. Here, we document our senior design project: designing a novel sorbent-based oxygen production process using mixed ion-electronic conductors which offer near-perfect selectivity to oxygen. This technology has not yet been realized commercially but could one day offer extremely pure streams of oxygen for use in medical, industrial, and aerospace applications.

We have conducted a survey and sensitivity analysis of the sorbent technology and identified key areas for further improvement to the technology. Analyzing both today's proven kinetics and tomorrow's potentially-realizable kinetics, we present a profitability analysis of the proposed plant producing a target of 30 tons per day of 99.99% pure oxygen.

Based on an oxygen selling price of $40 per ton, the realized process would operate at a loss in today’s economy. The total capital investment of the plant would be $1.1 million, and the expected NPV -$87,000. The estimated IRR is -28.08%, and the 3-year ROI is -7.4%. Break-even could be achieved if the selling price of oxygen rose to $56.70/ton. Enhancements to MIEC adsorption and desorption rates, by a factor of 10, would also achieve break-even economics. Such new class of improved MIEC perovskite-based sorbents would be good a good candidate for future commercialization.

Sincerely,

_____	_____
Chandler Dorris	Eric Lu
_____	_____
Sangjae Park	Fabian Toro

2. Introduction

2.1 Overview

The consumption of high-purity oxygen by the steel, medical, and chemical industries amounts to 1.2 million tons per day [HighBeam, 2016]. Currently, there are three commercially-realized processes for the production of oxygen: cryogenic, zeolite-based vacuum pressure swing adsorption (or VPSA), and ceramic-based oxygen transport membranes (OTM). This project studies the viability of using new mixed ionic-electronic conducting (or MIEC) materials as sorbents to produce 99.99% pure oxygen in a medium-scale, 30 ton/day plant.

Current research into the performance of MIECs indicates these materials may be more effective at separating oxygen from air than the current sorbents used in VPSA plants [Lemes-Rachade, 2014]. Therefore, this report aims to evaluate whether MIECs can be incorporated into a VPSA system that produces nearly pure oxygen at a competitive price point, and whether this system would result in an economically viable project. This project will focus on evaluating the conditions (pressure and temperature) where MIECs operate.

The MIEC technology presented in this report is not available for immediate use. We have assumed the properties of MIECs based on cutting-edge research [Lemes-Rachade, 2014] not yet available publicly. The goal is to provide an overview of the potential of MIEC technology and set possible benchmarks for material science researchers developing MIECs. Ultimately the report will provide conditions at which the technology can be implemented in competitive oxygen purification systems.

2.2 Project charter

Project name: High-Purity Oxygen Production Using Mixed Ionic-Electronic Conducting Sorbents

Project team: Chandler Dorris, Eric Lu, Sangjae Park, Fabian Toro

Project supervisors: Dr. Talid Sinno, Dr. Matthew Targett, Prof. Leonard Fabiano

Specific goals: Design an oxygen production system using Mixed Ionic-Electronic Conductors (MIECs) as sorbents in order to produce high- purity oxygen at a competitive price. Describe MIEC performance requirements of such a plant.

Project scope: *In scope*

- Design a process to produce 30 metric tons of 99.99% pure oxygen per day using MIEC sorbents
- Obtain material properties of MIEC sorbents under development today (herein "*nominal properties"* of MIECs)
- Model MIEC sorbent behavior to obtain rate of oxygen production under different material properties
- Analyze effect of operating conditions (pressure, temperature, and flowrate) on the rate of oxygen production
- Provide comprehensive economic analysis of conceived process, optimizing operating conditions to produce the most profitable plant
- Outline specific benchmarks that MIEC technology needs to meet

Out of scope

- Manufacture of MIEC sorbent
- Air pre-treatment (e.g. filtration)
- Oxygen delivery and storage

Deliverables:

- Process design with mass & energy balances
- Economic feasibility analysis
- Technical feasibility assessment

Timeline:

- February 2: Preliminary background material
- February 23: Base case and process flow diagram
- March 15: Detailed equipment design for a key process unit
- March 22: Major equipment designed
- March 29: Finances completed
- April 5: First draft of written report
- April 12: Final draft of written report
- April 19: Oral design report presentation

2.3 Project Motivation

MIEC materials are reported to be perfectly selective to oxygen and are capable of adsorbing large quantities of it [He, 2009]. Therefore, they hold the potential to produce 99.99% oxygen at a scale to meet industrial demands.

2.3.1 Comparison of Oxygen Production Systems

Currently three commercial systems exist for the production of high-purity oxygen, each of which has its own advantages and disadvantages. They each cater to different market segments. A description of each technology is presented below.

Cryogenic separation takes advantage of the difference in boiling points of oxygen and nitrogen (the largest component of air). By operating at cryogenic temperatures (approximately -210℃), it is possible for nitrogen to be distilled from air. Cryogenic separation is widely used in industry because of its ability to produce large quantities of high-purity oxygen. It is commonly the source of oxygen for the steel industry, since this industry requires very high volumes of high-purity oxygen. As we can see from this process's flowsheet (Figure 2.3.1), cryogenic production of oxygen requires a significant number of components, including various compressors, heat exchangers and separation columns. This makes the system expensive to purchase as well as operate. In order for it to be economically viable, the system needs to produce upwards of 200 tons per day of oxygen [Sirman.J, 2005]. Therefore, its main drawback is its inability to cater to market segments that require more

modest volumes of high-purity oxygen. Nevertheless, cryogenic separation is the most attractive option for commercial metal production because of its ability to produce large quantities of oxygen needed. The distillation of air at cryogenic temperatures can also provide high quality argon. Argon is essential for the production of steel; therefore, the steel industry benefits from using cryogenic systems to produce their oxygen.

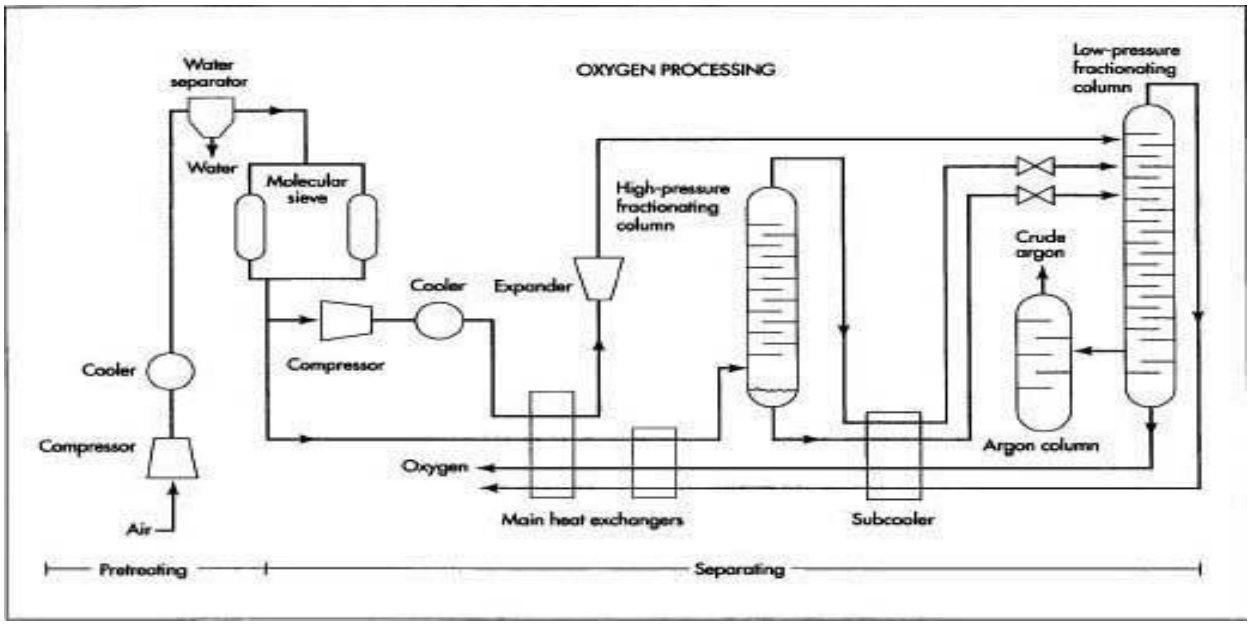

Figure 2.3.1: Process flowsheet for cryogenic plant

Oxygen transport membrane (OTM) separation uses membranes that selectively separate oxygen from nitrogen in air. It produces smaller quantities of high-purity oxygen, suitable for segments such as the medical industry. Nevertheless, this system comes with its own set of drawbacks. First, these membranes are expensive. Second, because they are made from ceramic materials they are also very fragile and prone to leaks if not handled with proper care [Kelly, 2014]. This can result in significant process downtime. Overall, the simplicity of a membrane separation unit comes with its own set of tradeoffs, such as high operating pressures (ranging from 3.5 to 30 atm absolute [Kelly, 2014]) and significant maintenance costs [Ashcraft. B, 2007].

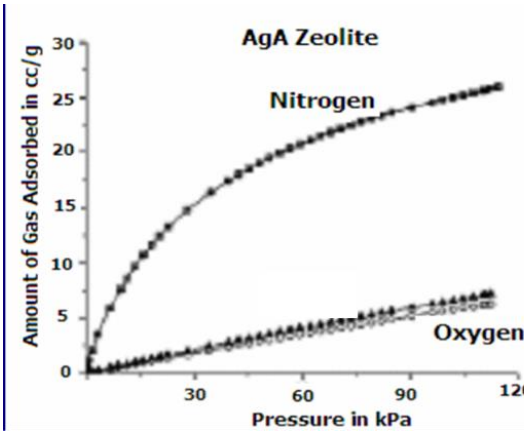

Figure 2.3.2: Silver ion zeolite adsorption Isotherms [Ashcraft, 2007]. This figure highlights the difference between oxygen and nitrogen selectivity.

Vacuum pressure swing adsorption (VPSA) systems are the most common oxygen purification systems in the market for onsite production of high-purity oxygen [Sirman.J, 2005]. These systems consist of columns packed with silver ion zeolites, microporous crystalline structures that selectively adsorb nitrogen. The packing behaves as a molecular sieve which adsorbs nitrogen, removing it from air. The adsorbed nitrogen is subsequently desorbed by decreasing the system's pressure by vacuum, which constitutes the second part of an adsorption/desorption cycle. Figure 2.3.2 depicts the adsorption isotherms of silver ion zeolites. From the graph, it is clear that the VPSA system cannot produce pure oxygen even though the difference in oxygen-nitrogen selectivity is substantial.

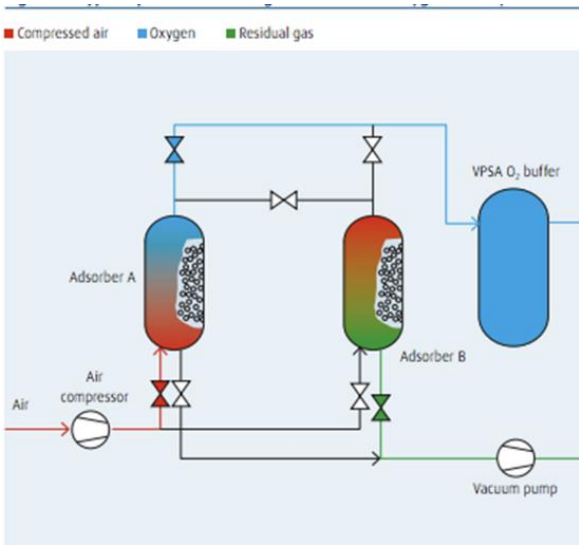

Figure 2.3.3: VPSA process flowsheet [Linde AG]. This diagram depicts the staggering of the columns in order to always have one column adsorbing while the other desorbs.

Figure 2.3.3 provides a brief overview of the process flowsheet, through color gradients in the adsorber columns the figure highlights the staggered operation of the columns. It shows the system operates always have one column with a*n* oxygen output and the other with a nitrogen output. If we compare it to Figure 2.3.1, we can see that a VPSA system requires significantly less equipment to operate.

VPSA systems using zeolites are commonly used since they appeal to a more varied segment of the oxygen consumption market. Their wide oxygen production output range and comparatively small capital cost are advantages compared to cryogenic systems.

2.3.2 Description of Zeolites

Zeolites are microporous crystalline structures that selectively separate molecules based on their size and polarity. Currently, the most common type of zeolite used in the air separation industry is silver ion zeolites (see Figure 2.3.4). These materials are used in pressure swing systems because, under different pressures, they are able to deform in order to adsorb specific compounds. Figure 2.3.5 shows a lattice of silver ion zeolites adsorbing nitrogen. Usually, the minimum pressure for a silver ion zeolite to adsorb nitrogen is 1.5 atmospheres absolute. When the zeolite is saturated with nitrogen, the pressure can be decreased to atmospheric pressure, allowing the zeolite to regain its original shape [Hutson. N.D, 2000]. As the zeolite regains its original shape, it will release adsorbed nitrogen. This process is called *regeneration*, because the interstitial spaces become empty and are again able to adsorb nitrogen in the next cycle.

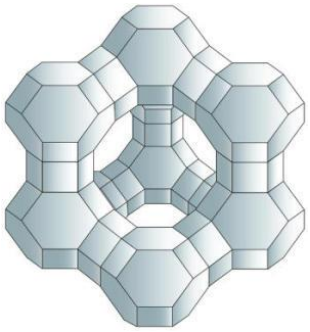

Figure 2.3.4: Silver ion zeolite structure [Hutson. N.D, 2000]

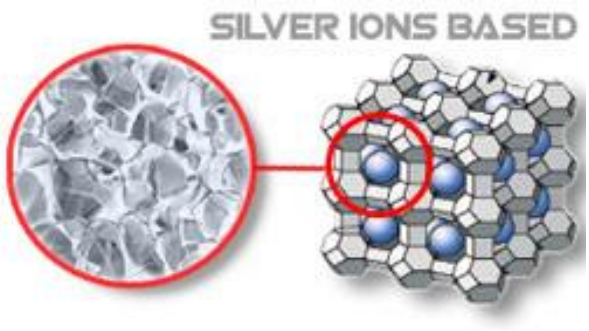

Figure 2.3.4: Silver ion Zeolite acting as molecular sieves, adsorbing nitrogen [Ashcraft. B, 2007]

By decreasing the pressure for the regeneration stage of the process using a vacuum, the operator is able to decrease the time and increase quality of the regeneration process,

which improves the overall efficiency of the cycle. Current systems are capable of recovering 62.74% of the available oxygen in the inlet air, with an average cycle time of 2.5 minutes [Ashcraft. B, 2007].

2.3.3 Description of Mixed Ionic-Electronic Conductors

MIECs in this paper refer specifically to a family of materials called perovskites which are the most suitable for oxygen purification [Ellet, 2009]. Perovskites have a general formula of ABO_3 where A and B are a variety of metal ions. Figure 2.3.6 shows a three-dimensional model of a perovskite composed of Strontium (Sr) and Titanium (Ti) in the A and B sites. Perovskites effectively separate oxygen because of their characteristic transition into a "brownmillerite" phase.

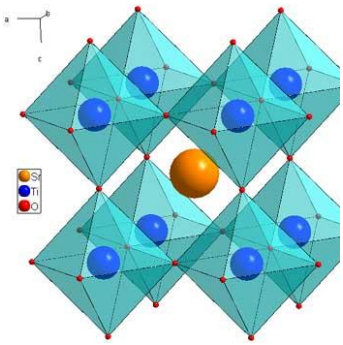

Figure 2.3.5: Strontium & Titanium perovskite structure [He, 2009]

The brownmillerite phase has a structure which consists of atomically ordered one dimensional oxygen vacancy channels instead of the three-dimensional tetrahedral structures exhibited by the perovskites at lower temperatures (see Figure 2.3.7) [Hyoungjeen, 2013]. This phase change is brought about by an increased temperature, which is highly desirable because ABO_3 turns into $ABO_{3-\delta}$. δ refers to the oxygen ions which leave the lattice. The oxygen ions leave interstitial space for molecular oxygen to be adsorbed

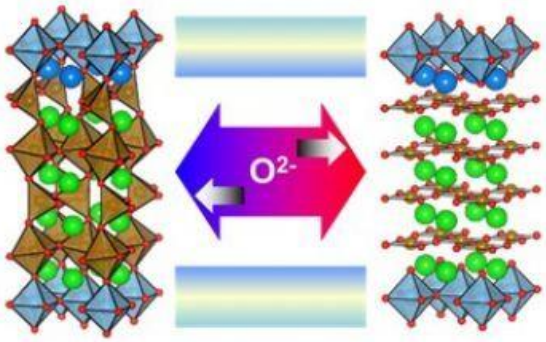

Figure 2.3.6: Transition of perovskite to brownmillerite phase [He, 2009]. This figure depicts the structural changes that occur when the perovskite transitions into the brownmillerite phase

from the air. δ depends on the choice of A and B metal ions [Ellet, 2009], and by selecting a material with high δ, the amount of oxygen adsorbed is greater.

In our design, MIECs will be incorporated in a VPSA system. There have been attempts at using MIECs in OTM systems [Sunarso, 2008], but due to the drawbacks of OTM, it was decided not to pursue that option. In order to use MIECs in a VPSA system they will be loaded into adsorber/desorber columns, analogous to a zeolite system. In order to do this, the MIECs will be pelletized by a ceramic solid state reaction [Eciija, 2012], whereby they will be mounted onto a porous ceramic substrate ~10 mm in diameter that can then be packed into the column.

2.4 Innovation Map

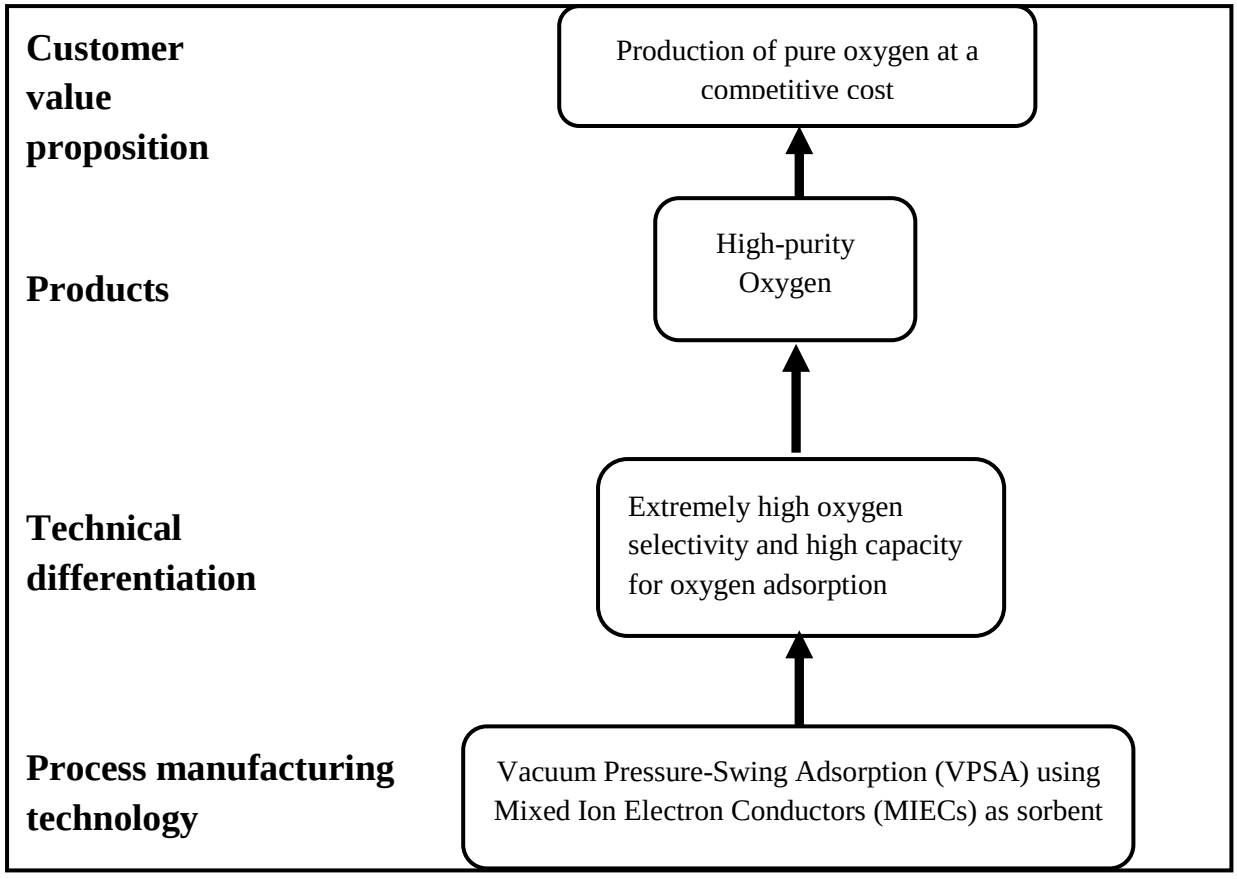

Figure 2.4.1: Innovation map for the production of oxygen using MIECs.

The possible use of MIECs in the oxygen production industry may provide a significant improvement over the current adsorbent technologies. MIEC materials have a competitive edge over silver zeolites because of their extremely high selectivity to oxygen. They are impervious to many impurities, unlike their zeolite counterparts. Given that oxygen consumers prize both competitively-priced and high-quality oxygen, MIECs hold potential to deliver. The other main advantage of using MIECs as sorbents in a VPSA system is that they have a high capacity for oxygen adsorption making them more efficient at capturing the available oxygen in the inlet air. This oxygen capture efficiency would decrease the volumetric flow of air required to flow through the columns.

3. Concept Stage

3.1 Market Analysis

The industrial gas market is valued at $9.1 billion as of 2015 [Morea, 2015], out of which the oxygen industry makes up 8.7% (see Figure 3.1.1). This industry caters to a wide variety of different segments including industrial manufacturing, chemical production, healthcare and research. The two main consumers of high-purity oxygen are the steel industry and the chemical industry, which includes agrochemicals, refineries, pharmaceuticals, polymers, pigments and oleochemicals. The steel industry consumes 48% of the total global oxygen output, whereas the chemical industry comes in at around 19% [HighBeam, 2016]. It is also very important to note that 40% of this oxygen being consumed is produced on site [HighBeam, 2016].

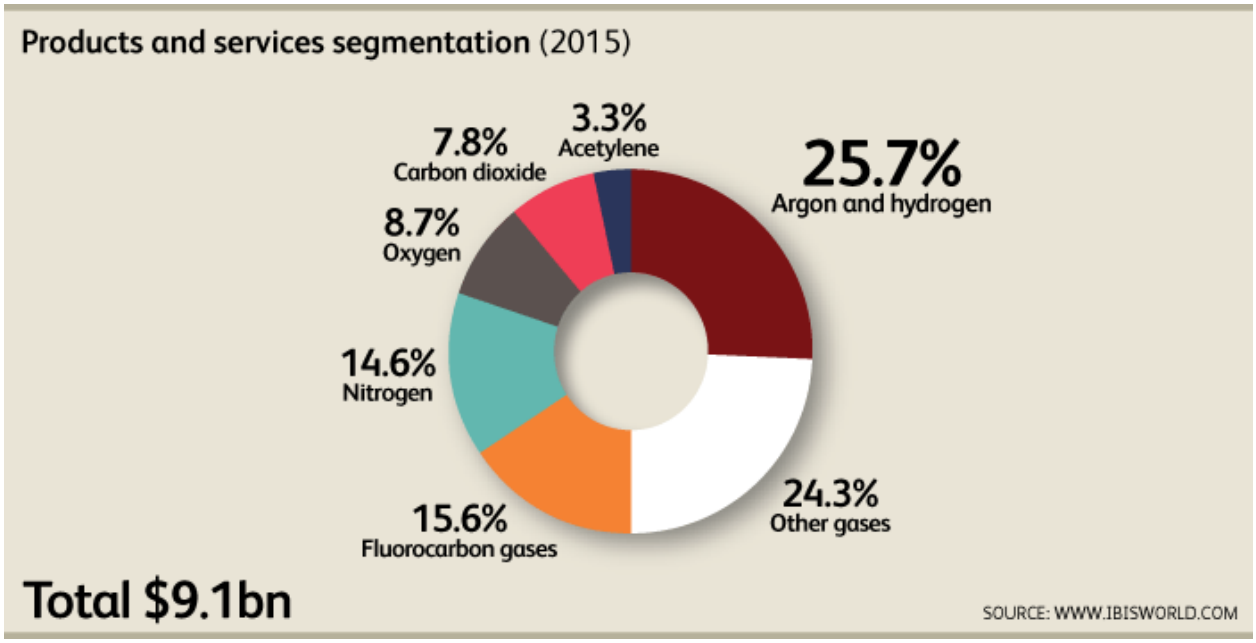

Figure 3.1.1: Industrial gas market breakdown [Morea, 2015]

3.2 Competitive Analysis

The VPSA system using MIEC will produce 30 tons of oxygen per day. This value was chosen because it falls within the output range of current VPSA systems in the market. Figure 3.2.1 show that current VPSA systems operate in the range of 10-200 tons per day or oxygen. It also shows that higher production output infringes on the cryogenic oxygen market share. This is because the main consumers of cryogenic are steel manufacturers that also value the argon the cryogenic systems provide. Table 3.2.1 lists the production specifications of the current VPSA systems in the market. A 30 ton per day out put clearly falls within the range of all of the commercial systems.

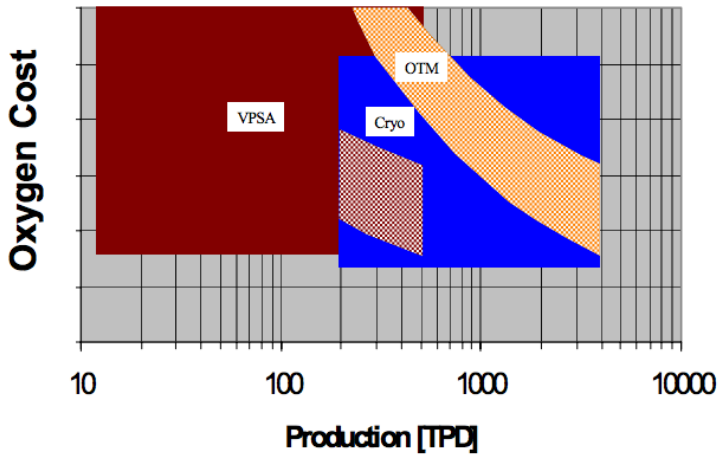

Figure 3.2.1: Cost vs Production graph for different technologies [Sirman.J, 2005]

Table 3.2 1: VPSA oxygen producers [Linde AG, Praxair,2013-2016, Chart Industries, 2016]

Main Competitors	O2 purity	Rate of production (metric tons per day)
Praxair	94%	30-200
Linde	90-95%	10-342
AirSep	94%	0.007-120

Table 3.2.2 provides a cost breakdown of the pricing for different oxygen production mechanisms, our technology will focus on competing with onsite production systems, since these hold a large market share and are the most cost effective systems for consumers downstream.

Table 3.2 2: Prices of commercial sources of oxygen [Sirman.J, 2005] [Rao.P, 2007]

Oxygen Supply	Manufacturing Technology	Price (per metric ton)
Pressurized cylinders	VPSA	$4,300-21,400
Liquid dewar	Cryogenic	$1,000-2,143
Bulk liquid	Cryogenic	$214-1,000
On-site production	VPSA	$24-40

4. Process Flow Diagrams and Material Balances

4.1 Overall Process Flow Diagram

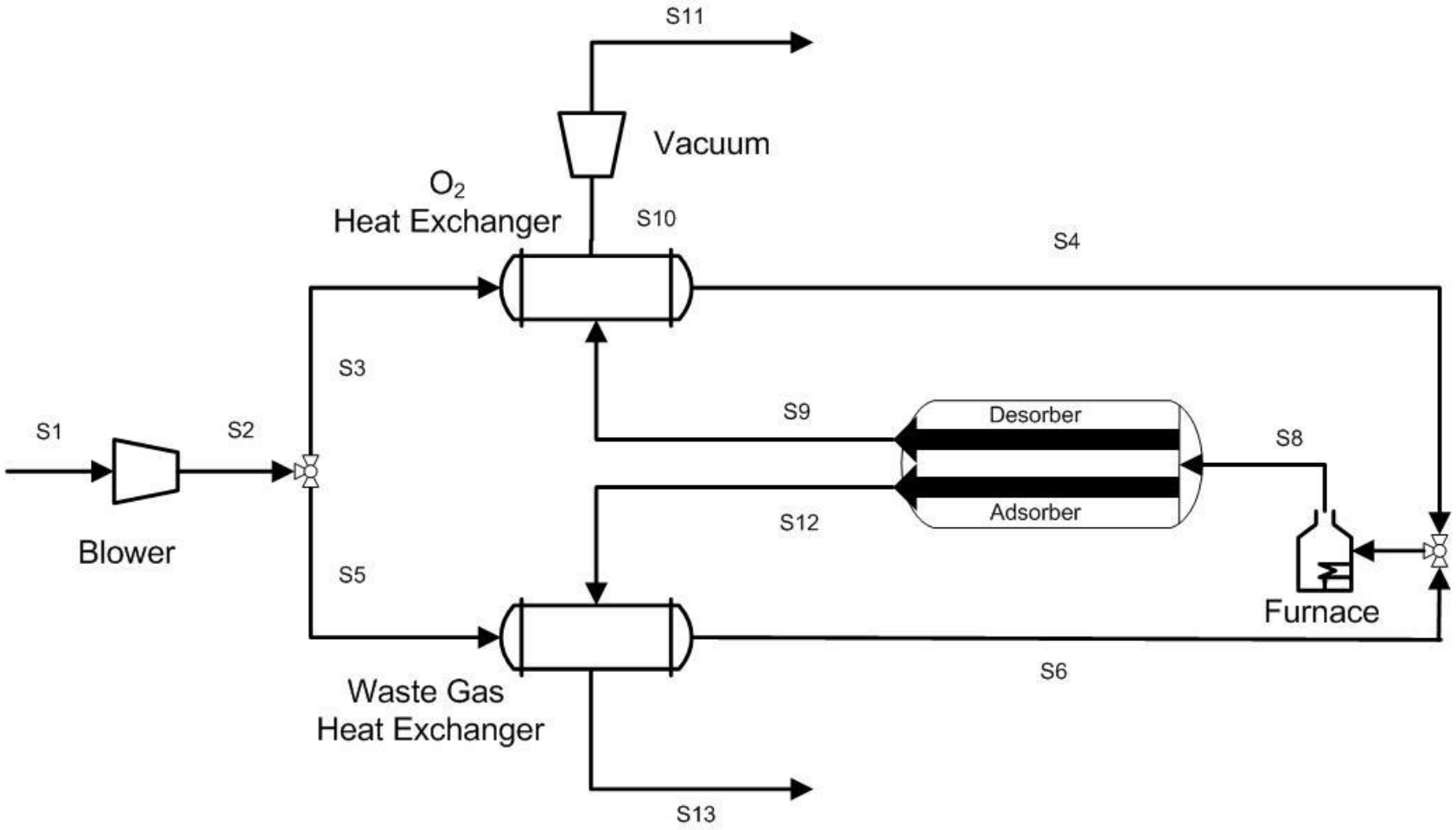

Figure 4.1.1: Overall process flow diagram for the proposed separation of oxygen from air by MIEC adsorption

4.2 Energy and Mass Balances

Table 4.2.1: Stream Properties

	S1	S2	S3	S4	S5	S6	S7	S8	S9	S10	S11	S12	S13
Temp (°C)	25.0	75.3	75.3	269	75.3	440	400	500	500	81.9	81.9	500	150
Mass Flow [kg/s]	3.14	3.14	0.73	0.73	2.41	2.41	3.14	3.14	0.35	0.35	0.35	2.79	2.79
Mole Flow [mol/s]	108	108	25.3	25.3	83.2	83.2	108	108	10.8	10.8	10.8	97.6	97.6
Pressure (atm absolute)	1.00	1.55	1.55	1.50	1.55	1.50	1.50	1.50	0.20	0.17	1.00	1.19	1.18
Volume Flow [m^3/s]	2.65	2.00	0.47	0.75	1.53	3.24	3.99	4.59	3.44	1.90	0.32	5.20	2.87
Mass Frac. of Oxygen	0.23	0.23	0.23	0.23	0.23	0.23	0.23	0.23	0.99	0.99	0.99	0.14	0.14

5. Process Description

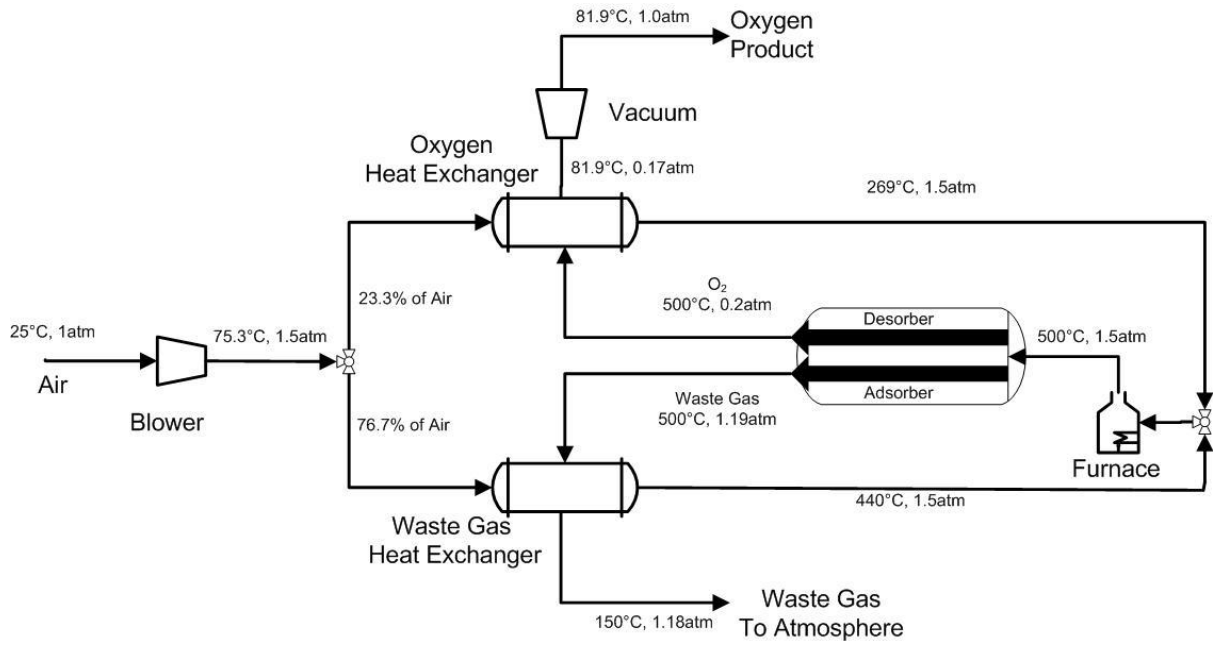

Figure 5.1.1: Process flow diagram displaying temperature and pressure across the process.

NB: All pressures are absolute pressures unless otherwise stated.

5.1 Overall Process Description

Air entering the process from the environment at standard atmospheric conditions (25℃ and 1 atm) gets compressed by a centrifugal blower which increases the stream's pressure to 1.5 atm. The air's temperature also rises to 75.3℃ as a result of the compression. The inlet stream then split into two streams, entering two shell-and-tube heat exchangers in parallel. 23.3% of the air enters the oxygen heat exchanger and exits at 269℃ and 1.55 atm. The other 76.7% of air enters the waste gas heat exchanger and exits at 440℃ and 1.5 atm. The air streams merge and pass through a furnace which heats the air up to 500℃. The air stream then enters the adsorption chamber at 500℃ and 1.5 atm.

In the adsorption chamber, oxygen is separated from air by adsorption onto MIECs. Inside the chamber are 59 tubes packed with MIEC pellets. The tubes cycle between adsorption and desorption. During adsorption, air flows through the tube, and oxygen is adsorbed onto the MIEC. The outflow is therefore oxygen-depleted air (mostly nitrogen),

which has been termed waste gas. The waste gas leaves the chamber at 500℃ and 1.19 atm. It is at a lower pressure than the inlet flow due to the removal of oxygen. Once the MIEC has been 95% saturated with oxygen, the tubes switches to the desorption mode. Air inflow is stopped, and the air remaining in the tube is pumped out by vacuum, lowering the pressure to allow oxygen to desorb from the MIEC. The outflow of desorbing tubes is the oxygen stream (S9). The adsorption cycle then repeats. Due to the large number of tubes which alternate adsorption and desorption phases, the outflow streams of the adsorption chamber are approximately in steady state. More information about the adsorption chamber can be found in Section 7, Equipment List and Unit Descriptions.

The shell-and-tube heat exchangers serve the dual purpose of heating the inlet air stream and cooling the outlet streams of the adsorption chamber. Both the oxygen and waste gas streams exit the adsorption chamber at 500℃ before entering different heat exchangers. The waste gas stream (S12) enters the waste gas heat exchanger to heat part of the air inlet flow. The waste gas enters the waste gas heat exchanger at 500℃ and 1.19 atm and exits to the atmosphere at 150℃ and 1.18 atm. The oxygen stream (S9) enters the oxygen heat exchanger so that it is cooled by part of the inlet air to 81.9℃. The oxygen heat exchanger was designed for near maximum cooling of the oxygen stream. The oxygen stream then enters a jet ejector vacuum. The vacuum lowered the pressure so that the oxygen would desorb from the MIEC. After the vacuum, the oxygen stream is sent off to the consumer at 81.9℃ and 1 atm.

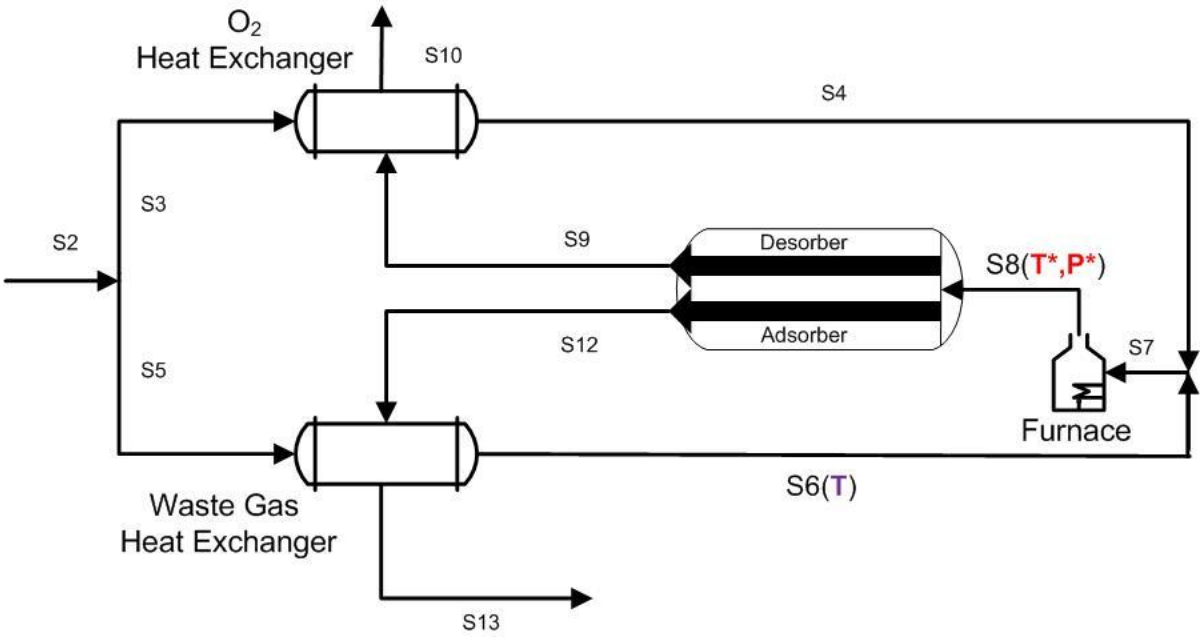

Figure 5.2.1: Heating and cooling block showing the variables for the total cost of heating optimization. For the purpose of optimization, the variables T* and P* (shown in red) are the inlet conditions to the adsorber and T (shown in purple) is the outlet temperature of the waste gas heat exchanger.

5.2 Heating Considerations

The purpose of the heating and cooling block (shown in Figure 5.2) has the dual purpose of heating the inlet air stream from atmospheric conditions of 25℃ to 500℃ and cooling the oxygen stream leaving the adsorption chamber. To accomplish this, two shell-and-tube heat exchangers and a furnace were used. The oxygen heat exchanger was designed for near maximum cooling of the oxygen stream due to requirements of the vacuum. The designs of the waste gas heat exchanger and furnace were determined by an optimization.

To decrease the cost of the vacuum, the oxygen heat exchanger was designed for near maximum cooling of the oxygen stream. The most critical function of the oxygen heat exchanger was to cool the oxygen stream leaving the adsorption chamber, both because sending oxygen to the consumer at 500℃ (the outlet temperature of the adsorber) is

impractical and because the cost of the vacuum increased with the temperature of the oxygen stream. The cost of the vacuum is dependent on the volumetric flowrate into the vacuum which is directly dependent on the temperature according to the ideal gas law. Although the cost of the heat exchanger increases as the outlet oxygen stream (S10) temperature decreases, the utility cost of powering the vacuum is much more expensive than the heat exchangers, so the cost of vacuum took priority. This is why the cost and outlet temperatures of the oxygen heat exchanger were not varied during the heating optimization. The minimum temperature approach was set at 6.67℃ (20℉) as recommended in Seider et. al for above ambient temperature shell-and-tube heat exchangers.

Table 5.2.1: Heating Optimization Variables

Variable	Definition
Heating Equipment	Waste gas shell-and-tube heat exchanger Oxygen shell-and-tube heat exchanger Furnace
Total Cost of Heating	Capital cost of heating equipment + Operating cost for the furnace
T*	Inlet temperature to the adsorption chamber
P*	Inlet pressure to the adsorption chamber
T	Outlet air temperature of the waste gas heat exchanger

To determine the size and outlet temperature of the waste gas heat exchanger, an optimization was performed on the total cost of heating, defined as the capital cost of the two heat exchangers and the furnace plus the operating cost over 10 years. Ten years is the life of our project, and the operating cost for the heating system is the cost of natural gas for the furnace assumed to be 4$/million BTU (Nasdaq, U.S. National Average Natural Gas Price).

The optimization was performed for various values of the inlet temperature and pressure to the adsorption chamber, referred to as T* and P*. The temperature (T) of the air outlet of the waste gas heat exchanger (S6) was varied and the total cost of heating was calculated for each T. The heat exchangers were designed and the cost estimated using Aspen Exchanger and Design Rating (EDR). The equations used to estimate the cost of the furnace are from Seider et. al and can be found in Appendix B.

The results of the optimization at P*=1.3atm and P*=3atm are shown in Figures 5.3 and 5.4. For all P*s and T*s, the total cost of heating decreased as T increased until T reached approximately 90% of T* when the cost of heating would increase sharply. Consequently, the minimum cost of heating for all T* and P* was when T was close to 90% of T*. In the process design chosen T*=500℃ and P*=1.25 atm, so the optimization showed that T=440℃ provides the minimum cost of heating.

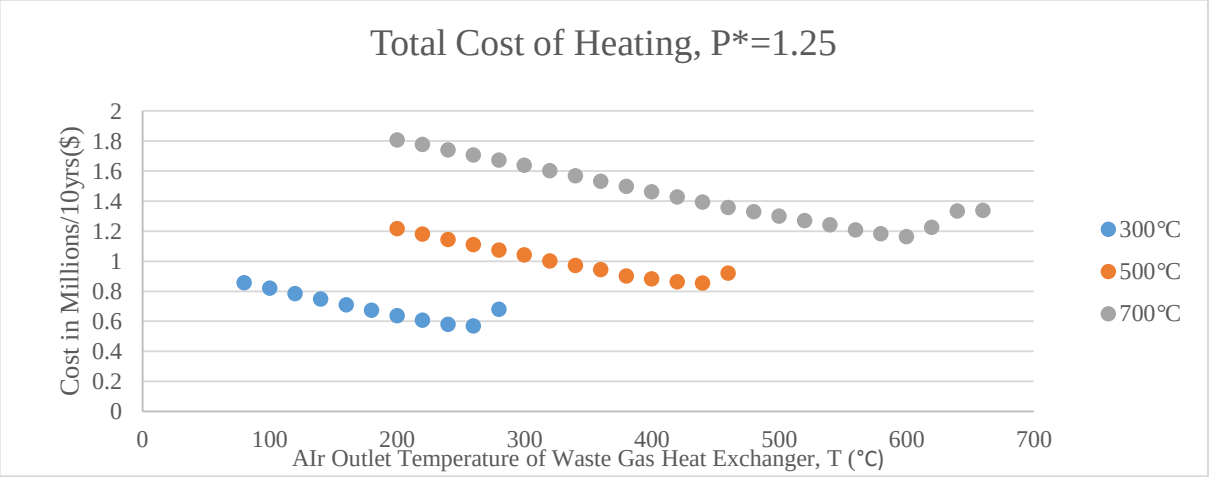

Figure 5.2.1: Total cost of heating over 10 years vs. the outlet air temperature of the waste gas heat exchanger (T). The total cost of heating is defined as the capital cost of the two shell-and-tube heat exchangers and the furnace plus the operating cost over 10 years. T* and P* are the inlet temperatures and pressures to the adsorber. The heating cost is a relationship based on how much heating is put on the heat exchangers versus the furnace. The temperatures that produce the minimum cost are 260℃, 440℃, and 600℃ for T* of 300℃, 500℃ and 700℃ respectively.

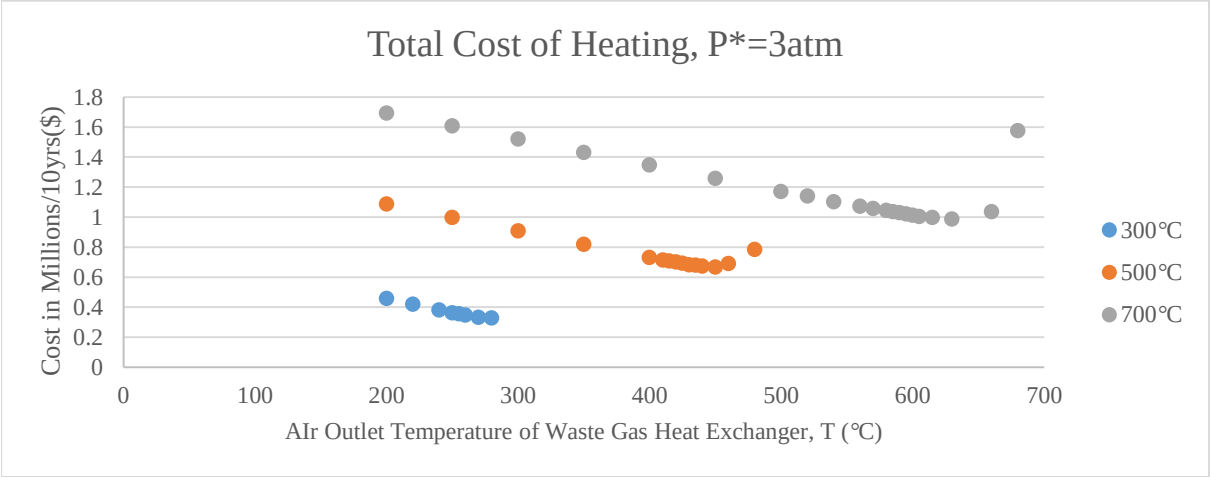

Figure 5.2.2: Total cost of heating over 10 years vs. the outlet air temperature of the waste gas heat exchanger(T). The total cost of heating is defined as the capital cost of the two shell-and-tube heat exchangers and the furnace plus the operating cost over 10 years. T* and P* are the inlet temperatures and pressures to the adsorber. The heating cost is a relationship based on how much heating is put on the heat exchangers versus the furnace. The temperatures that produce the minimum cost are 280℃, 450℃, and 630℃ for T* of 300℃, 500℃ and 700℃ respectively.

5.3 Process Control

The plant will be run through a distributed control system (DCS) using multiple sensors that enable remote monitoring and control. As the plant is not staffed, instrumentation will be connected to the internet for monitoring by ethernet cable. Indicators, sensors, feedback systems, and pneumatic controls are required to keep the plant under safe, steady operation while meeting its target production of 30 tons of oxygen per day. In particular, blower pump speed and furnace gas flow rate must be controlled closely to ensure reliable pressure and temperature operating conditions. Both must adjust to ambient pressure and temperature deviations, potentially unstable flows, and system leaks.

The purity of oxygen must also be guaranteed for customers. To that end, batch samples of oxygen from each of the 59 adsorption tubes will be sampled by gas chromatography every hour. Using statistical process control during startup, vacuum pump times and inter-cycle wait duration may be calibrated to guarantee oxygen purities greater than 99.99%. Expected purities of 99.99% and higher will pass test. Purities between 99.9 and 99.99% will trigger a warning condition that recommends operator action. Purities less than 99.9% from any tube will automatically trigger the DCS to take that tube offline until manual intervention, potentially requiring on-site diagnostics, can be executed.

Standard Operating Procedures

Crucial to the operation of every plant are a set of standard operating procedures (SOPs). A stand-in SOP for plant startup can be found in Appendix H.

6. Adsorption Column Modeling

6.1 Modeling Overview

An understanding of the operating principles behind the adsorption chamber is crucial to process design. Without an intuition for how quickly oxygen adsorbs and desorbs, cost optimization would be impossible.

Across similar operating pressures (1.25-2 atm absolute), temperatures (300- 500℃), and flow conditions, oxygen adsorption varies by magnitudes. In other words: **similar plant designs costing about the same produce very different amounts of oxygen**. Material properties of the MIEC, including oxygen capacity and its adsorption and desorption kinetic constants, strongly affect the rate of oxygen production. **These differences can be the difference between a net loss and gain from operating the plant**.

This section outlines simulations performed to optimize the rate of oxygen production in the adsorption chamber, a cylindrical column containing multiple, independent adsorption tubes. Assumptions are summarized in Table 6.1. Drawing upon knowledge from computer science, mathematics, and physics, this section sets the stage for later choices in optimizing process economics. After reading this section, one should be familiar with the design considerations, material properties, and chemical principles pertinent to the plant. Based on numerical modeling of the adsorption chamber over several parameters, we find those listed below most dramatically affect oxygen adsorption and desorption:

- **Operating temperature and kinetics**
- **MIEC density**
- **Flow rate**
- **Operating pressure**

Table 6.1: Summary of Assumptions Made in Simulations

Assumption	Justification
Ideal gas law	MIECs operate at ~700K and 1-10 atm where the ideal gas law is valid for air (the compressibility Z ~ 1) [Green 1984]
Plug flow of air	Interactions between air, the wall, and other air molecules are relatively unimportant, so all air entering the column at the same time is assumed to move together. The viscosity of air is small.
Radially-symmetric air flow in cylindrical tubes	Tubes and columns are typically cylindrical, and randomly-distributed packing is assumed to produce approximately radially-symmetric flow.
Negligible pressure drop across column from friction	MIEC pellets are large, and the Ergun equation shows pressure drop across the column < 0.5 atm due to friction. $\Delta P < 0.1$ atm in most cases conditions studied.
Linear driving force applies to MIECs	Empirical data provided for MIECs follows the LDF model, and fast transport of oxygen in MIEC-like compounds has been observed [Kim 1989].
Two components in air: oxygen and nitrogen	The molar fraction of oxygen in air is assumed to be 0.21. Other components of air, including water vapor, make up a small part of air on both a mass and molar basis (< 3%). Nitrogen can thus be assumed to be the only other component of air, with a mole fraction of 0.79.

6.2 Basic Considerations

As described in the preceding sections, porous mixed ionic-electronic conducting pellets selectively bind to oxygen from air. Earlier works [Sunarso 2008, Hyoungjee 2008] have shown the amount of oxygen per volume of MIEC[1] is governed by an isotherm (detailed later) dependent on pressure and temperature. As a result, the pressure, P_{in} [atm], and temperature, T_{in} [K], of air entering the column affect the maximum amount of oxygen each

pellet can adsorb, q^* [mol/kg sorbent]. We will see q^* *strongly* affects the rate of oxygen production.

At or before oxygen adsorbed onto the MIECs saturates to q^*, the air inlet must be shut off and oxygen desorbed before more oxygen can be adsorbed. The process of adsorption and then desorption step is known as a *cycle*. A typical cycle showing the rise and fall of oxygen adsorbed by the MIEC pellets is illustrated in Figure 6.1.1.

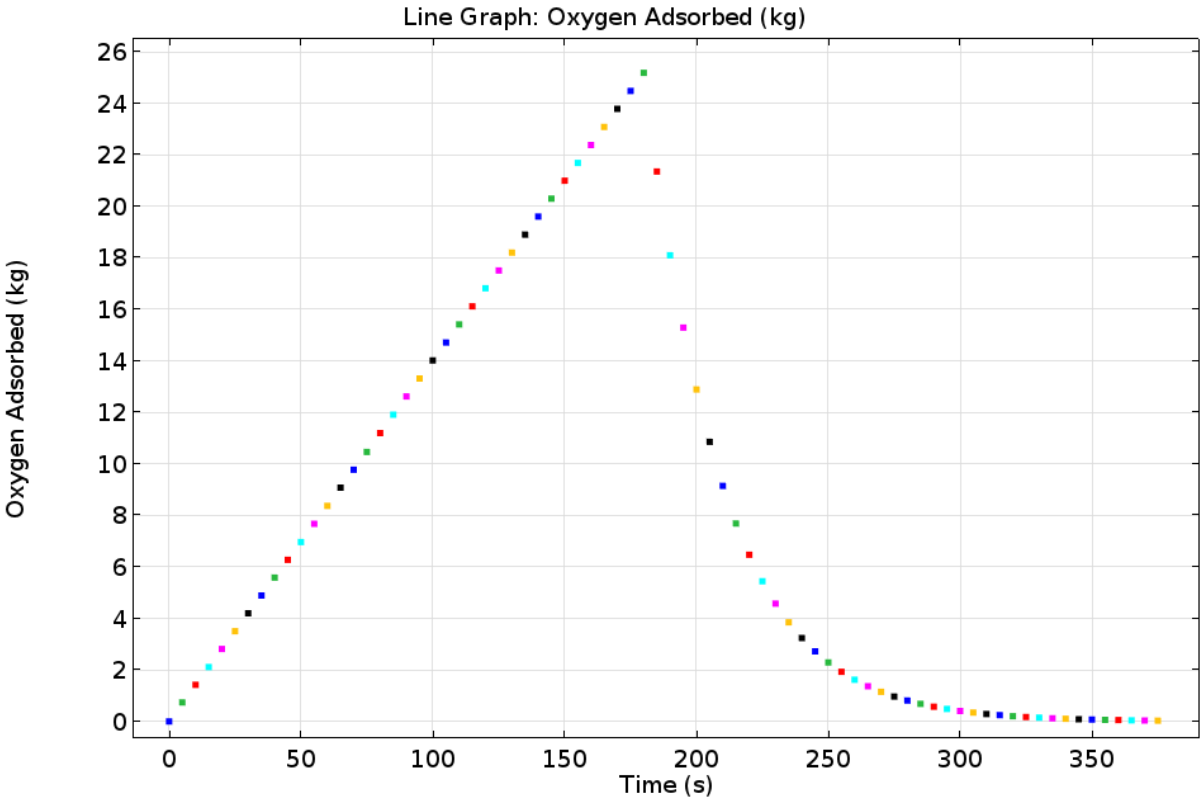

Figure 6.2.1: Typical curve of oxygen adsorbed by MIEC, with cycle starting at $t = 0$. Oxygen adsorbed is obtained by integrating $q(z,t)$ at a particular time over the volume of the adsorption chamber.

Cycle times should be short to reduce the number of tubes and thus cost required by the process. To keep cycle times short, the rate of oxygen adsorption must be as high as possible.

[1] We assume the entire pellet volume is active, which is true provided the diffusion rate of oxygen from the surface through the volume is faster than the rate of adsorption and the material has an isotropic internal distribution of active sites.

Pellets are to be well-distributed throughout the column to maximize the volume over which adsorption can occur. Air bypassing the main volume of sorbent is undesirable – some oxygen would have no opportunity to adsorb in that case. Accordingly, air flow is designed to be steady and uniform through the sorbent. We additionally assume radially-symmetric plug flow where air advances in a series of fronts. Column packing is randomly distributed, so flow velocity and oxygen adsorption should not depend on radial position. These assumptions enable 1-D simulation of adsorption behavior, greatly simplifying the study of the 3-D column without loss of accuracy. Studying the details of fluid flow in 3-D would require a solver such as Fluent [Ansys 2016] or SU2 [SU2 2016] for rigorous analysis.

Adsorption Kinetics

Sorbent capacity is important in determining the rate at which oxygen adsorbs throughout the adsorption chamber. This results from the **linear driving force** (**LDF**), which relates (1) the concentration of oxygen in the gas phase and MIEC to (2) how quickly adsorption occurs. Although the rate of adsorption fundamentally depends on thermodynamic properties of the active material and the gas (diffusivity and difference in chemical potential) *the assumption that the transport resistance of MIEC pellets is small* resembles cases where the LDF model applies well (Sircar and Hufton). Accordingly, we argue the LDF model is suitable to study MIEC sorbents.

In the LDF model, oxygen gas entering the column just after the completion of desorption sees several MIEC sites available for adsorption. However, the number of surface sites decreases once more oxygen is adsorbed, so oxygen entering long after the cycle adsorbs slower. Mathematically, this "difficulty" to find an adsorption sites is described as:

$$\frac{dq(z,t)}{dt} = k(P,T)[q^*(P,T) - q(z,t)] \tag{6.1}$$

$\frac{dq}{dt}$ = rate of oxygen adsorption, having units $\frac{mol}{kg\ s}$

$k =$ kinetic constant of adsorption or desorption, dependent on pressure (a function of position and time), temperature, having units s^{-1}

$q =$ oxygen adsorbed at position z and time t, with units mol/kg

$q^* =$ oxygen sorbent capacity, dependent on pressure and temperature, with units mol/kg

From equation (6.1), one can conclude the rate of oxygen adsorption $\left(\frac{dq}{dt}\right)$ decreases as time goes on and q increases. q^* may initially increase across the column as pressure builds ($q \cong 0$ at the start of each cycle), but it will eventually saturate to the maximum capacity for the process inlet temperature and pressure.

Today's fastest-adsorbing MIECs have shown $k \cong 2 * 10^{-2}\ s^{-1}$ at 500℃.

6.3 MIEC Oxygen Capacity Isotherm

The sorbent capacity q^*, from equation (6.1), results from the equilibrium concentration of oxygen between the gas phase and MIEC. This relationship is known as an *isotherm*. Oxygen bound to the MIEC acts as an inactive site so that:

$$A + O_2 \leftrightarrow A_{ads} \tag{6.2}$$

In equation (6.2), A is a free MIEC site while $A_{ads}$is a site with oxygen adsorbed. Oxygen in the gas phase, O_2, can reversibly adsorb or desorb based on temperature and pressure conditions. Based on projected experimental data expressing the isotherm, we model q* as:

$$q^* = (-8.355 * 10^{-4}\ T + 1.345)[0.0876 \ln(P_{O2}(z) + 1.1343] \tag{6.3}$$

where T is the temperature and P_{O2} is the partial pressure of oxygen at position z and time t.

Figure 6.3.1 plots q^* as a function of P_{O2} for a number of potentially realizable operating temperature of MIECs. **Between 1 and 10 atm air pressure at 500℃, the sorbent capacity rises only 20% though blower costs are expected to rise exponentially.**

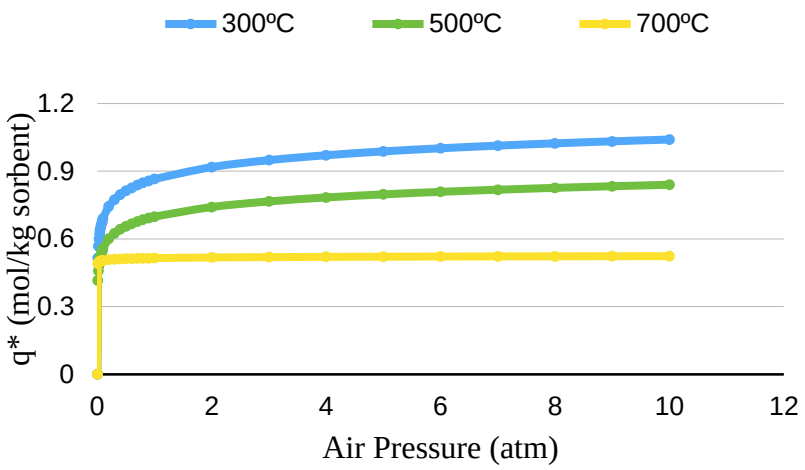

Figure 6.3.1: Sorbent oxygen capacity vs. gas-phase pressure of air. As a logarithmic function, the rise is very slow past 1 atm. Oxygen partial pressure is 0.21 times air pressure.

At 700℃, the change of q^* between 1 and 10 atm air pressure is even smaller: only 1%. The pressure dependence of sorbent capacity is thus weak but not entirely negligible.

6.4 Desorption Kinetics

The linear driving force from (equation 6.1) describes the rate of oxygen transfer between the MIEC and gas phase both for adsorption and desorption. In the case of adsorption, we assume the kinetic term is constant; however, for desorption, the rate was found to vary logarithmically with the inverse of oxygen pressure, P_{O2}:

$$k_{dsp}[\,s^{-1}] = 1.6 * 10^{-3}\, s^{-1} * \ln\left(\frac{0.21}{P_{O2}}\right) \tag{6.4}$$

The relationship between the kinetic constant of desorption and partial pressure of oxygen in the chamber is plotted in Figure 6.4.1:

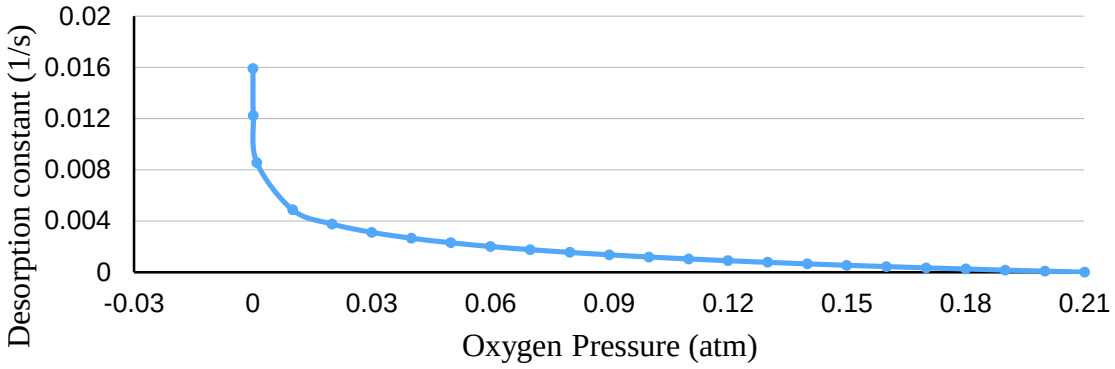

Figure 6.4.1: Desorption coefficient vs. pressure of oxygen, from equation (6.4).

This low k_{dsp} at ambient pressures (0.21 atm) is what requires the purge cycle: without pumping out the air that was flowing through the column, no desorption occurs. Desorbing oxygen at a pressure of 0.2 atm results in an extremely slow desorption rate approximately 10,000 times smaller than the rate of adsorption ($k_{dsp} \approx 10^{-6}\, s^{-1}$). Only at 10^{-6} atm, ~1 mTorr, does the desorption constant become comparable to the adsorption constant.

Beneficially, q is large at the start of the purge cycle and q^* approaches zero at low pressures. Still, the rate of *desorption is expected to be quite slow*.

6.5 Transport Equations

From the above information about oxygen adsorption/desorption and column capacity, the behavior of oxygen in the column can be solved. Adsorption and desorption rate, MIEC density, temperature, pressure, and flow rate are found to be sensitive operating parameters that affect the rate at which oxygen is produced.

Airflow through column

We assume the pressure drop due to friction on air flowing through the column is negligible. By supposing a constant entry velocity of air at ~1 m/s, under 1-D, pseudo-steady state, radially-symmetric plug flow through a cylindrical column such that the Ergun equation (equation 6.5) applies, we determine the pressure drop is indeed small, about 0.2 atm for typical pellets of MIEC which have a radius of 5 mm. Indeed, air has a low viscosity relative to, e.g. water. Based on our guiding heuristic that air compressors cost a lot to operate, flow rate and pressure increase should be small. Indeed, we see low pressure drops from friction at low flow rates, validating our assumption pressure drop due to friction through the column is small. Pressure drop from consumption will be seen to be much larger.

$$\frac{dp(z)}{dz} = \frac{150\mu(1-\varepsilon)^2 u}{\varepsilon^3 d_p^2} + \frac{1.75(1-\varepsilon)\rho u^2}{\varepsilon^3 d_p} \tag{6.5}$$

$p(z)$ = pressure drop
L = height of the bed
μ = fluid viscosity
ε =void fraction
u_0 = fluid superficial velocity (the velocity before the packing)
d_p = particle diameter
ρ = density of air

Transport

The concentrations of gas flowing through the adsorption chamber can be described by the mass transport equation describing convection, diffusion, and consumption through a cylindrical vessel [Incropera 2011]. Under our assumptions, the 1-D equation for mass transport over time (t) and space (z) is given by equation (6.6):

$$\frac{\partial c_a}{\partial t} + u\frac{\partial c_a}{\partial z} + \left(\frac{\partial q}{\partial t}\right) - D_{AB}\left(\frac{\partial^2 c_a}{\partial z^2}\right) = 0 \tag{6.6}$$

c_a= concentration of species A, having units $\frac{mol}{m^3}$

D_{AB}= diffusivity of A in B

In our simulation, we track the concentration of oxygen (zA), diffusing through nitrogen (B) in the gas phase.

By the ideal gas law:

$$c_a = \frac{P}{RT} \tag{6.7}$$

Oxygen

Oxygen is adsorbed from the gas phase as described by equation (6.1):

$$\frac{dq}{dt} = k[q^*(z,t) - q(z,t)] \tag{6.1}$$

Nitrogen

As nitrogen does not react with the MIEC, which has infinite selectivity to oxygen,

Considerations for Simulation Input

The concentration of oxygen is given by the ideal gas law (equation 6.7) as function of temperature and pressure. As an example, at an operating temperatures of 500℃ and pressures of 1.5 atm, oxygen entering the column will have a concentration of:

$$c_{O2} = \frac{\dot{n}}{\dot{V}} = \frac{y_{O_2}P}{RT} = 4.97 \text{ mol/m}^3 \quad (6.8)$$

This inlet concentration serves as a boundary condition for equation (6.6).

An open boundary condition also specifies oxygen cannot backflow and the gradient is zero across the boundary:

$$\nabla c_{O2} = 0 \quad (6.9)$$

The variable q* must also be tracked along the length of the column to accurately track the quantity $\left(\frac{dq}{dt}\right)$ adsorbed.

Solver

Solutions to the transport equation (6.6) were obtained using COMSOL Multiphysics, version 5.0. The study used an extremely fine mesh (corresponding to point elements 0.067 m apart from one another) and was set to produce a relative tolerance of 0.001. The model employed the chemical reaction module to track concentration of oxygen in the gas and MIEC. Numerous parameters were identified and entered into the model, described in the next section. Outputs from the simulation are also described. Appendix G shows selected images illustrating the use of COMSOL.

6.6 Parameters considered

Simulation Output: Number of tubes required

Simulation Input: Size of tube

The number of tubes is derived from the rate of oxygen adsorption over time, determined from the COMSOL simulation. Since equation (6.6) is 1-D, the rate of oxygen adsorption scales linearly with cross-sectional area. Area is proportional to tube radius squared. Tubes were designed with a length of 2 m, while area was constrained by a tube length-to-diameter ratio of 6. These values were selected heuristically to promote ease of handling and to ensure adequate heat transfer through the adsorption chamber. The output of a single tube was scaled until 30 tons/day of O2 was produced.

Simulation Input: Porosity of column

The porosity ε of the adsorption chamber filled with 10 mm-diameter cylindrical pellets is assumed to be 0.4, a typical porosity for well-packed spherical pellets in a column.

Simulation Input: Fraction of MIEC in pellet

Typical catalytic surfaces range from 0.3 to 0.7 in coverage by active material. 0.5 is used as a representative value for MIECs.

Simulation Input: Sorbent density

As illustrated by Table 6.2, numerous materials may operate suitably as an oxygen sorbent. The chosen material should have a high density to bring about a directly-related increase in oxygen adsorption.

Table 6.2: Candidate oxygen sorbent materials. Densities are tunable; typical/most common recorded density presented. Cost estimates are based by industrially sourcing raw materials [Alibaba, 2016] and multiplying by 1x and 100x to include preparation cost.

	Density (kg/m^3)	**Cost Range**
$CaTiO_3$	4,500	$2-200/kg
$SrTiO_3$	5,100	$3-300/kg
$La_{0.9}Sr_{0.1}Co_{0.1}Fe_{0.9}O_3$	6,300	$6 to 600/kg

Simulation Input: Adsorption constant and temperature

Increasing the adsorption constant decreases the time required for a cycle to approach saturation. Similarly, reducing temperature improves the capacity of each pellet, generally increasing the rate of adsorption.

Simulation Output: Mass of MIEC required

The cost of the MIEC material for the column over 10 years was determined by assuming a $40/kg capital cost. The minimum mass of MIEC sorbent for a particular plant design thus had to be calculated. It was found as the number of tubes times the volume of MIEC per tube times the density of the sorbent. The volume of MIEC per tube equaled the volume of each tube times the fill fraction times the fraction of MIEC per pellet.

Simulation Input: Desorption time

The time for desorption, based on desorption kinetics, influences cycle time and thus the number of columns required for oxygen production. The nominal MIEC desorption constant used in early simulations was far smaller than

Simulation Input: Air flow rate into column

Flowing more oxygen into the column at higher speeds allows for rapid convection of oxygen increasing the rate of adsorption.

6.7 Sensitivity of Parameters

By simulating over combinations of parameters listed in Section 6.6, the rate of oxygen production was identified. That value, combined with the operating conditions simulated, enabled the of creation heuristics guiding process optimization, e.g. decreasing *parameter x* increases the rate of oxygen production.

Temperature Sensitivity

Decreasing **temperature** increases the rate of oxygen adsorption. This is expected as lower temperature increases the sorbent capacity as shown in equation (6.3).

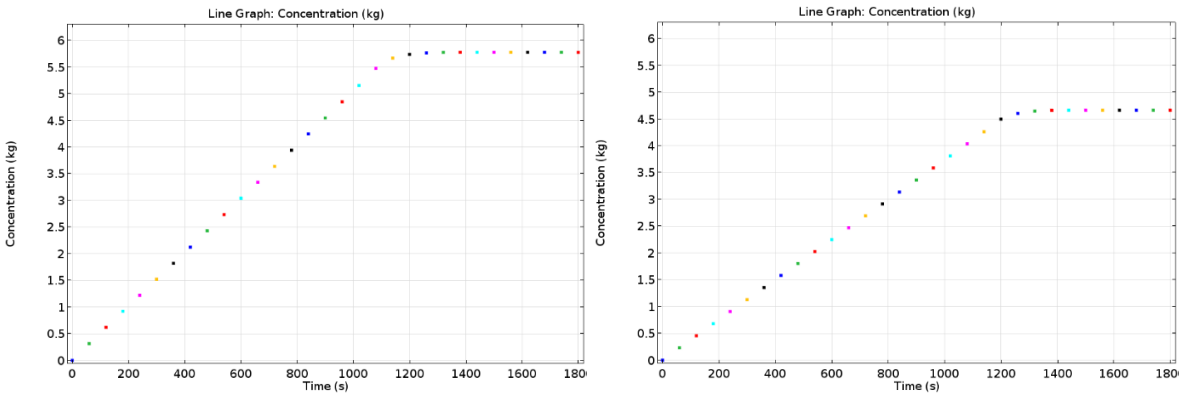

Figure 6.7.1: Adsorption behavior of oxygen at (a) 300℃ on the left and (b) 500℃ on the right. About 20% more oxygen is adsorbed per cycle at 300℃ than 500℃, 200s faster.

Pressure Sensitivity

Increasing **pressure** increases the rate of oxygen adsorption. This is expected as higher pressure increases the sorbent capacity as shown in equation (6.3).

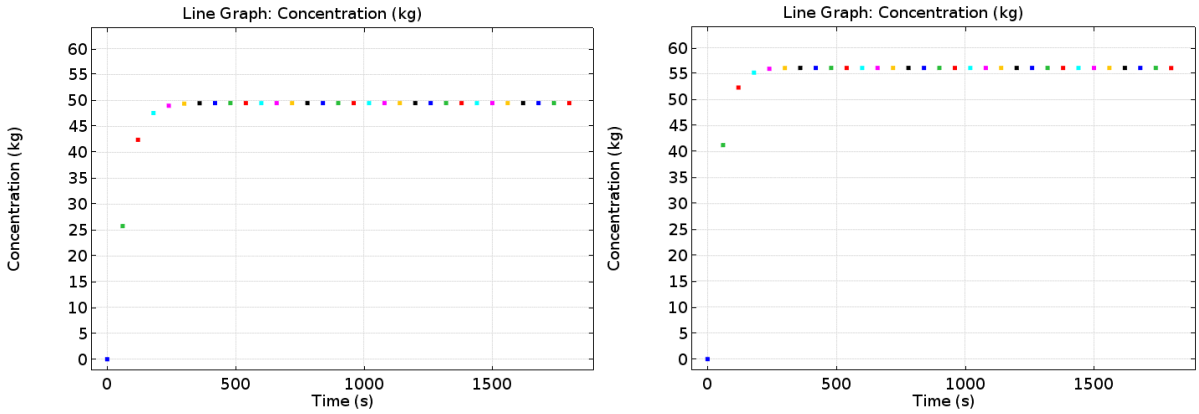

Figure 6.7.2: Adsorption behavior of oxygen at (a) 2 atm on the left and (b) 10 atm on the right. About 10% more oxygen is adsorbed per cycle at 10 atm than at 2 atm, though on comparable time scales. T = 500℃, air flow rate = 10 m/s.

Sorbent Density Sensitivity

The rate of oxygen adsorption is proportional to **density**. However, the cost of the MIEC material also scales directly with density. On the 30 metric ton/day scale, MIEC material with a density of 3,500 kg/m^3 are between $50-500,000 (operating costs will be higher in cases where MIEC cost is lower).

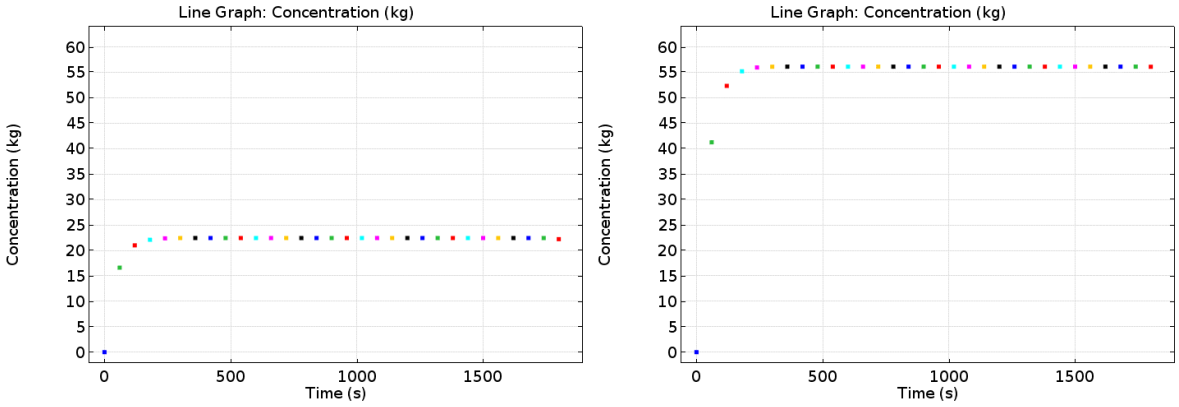

Figure 6.7.3: Adsorption of oxygen onto (a) 2000 kg/m^3 sorbent on the left and (b) 5000 kg/m^3 sorbent on the right. 5000/2000 = 2.5 times more oxygen is adsorbed per cycle with the 5000 kg/m^3 sorbent, in the same amount of time.

Flow Rate Sensitivity

Increasing **oxygen flow rate** significantly decreases cycle time, reducing the number of tubes and thus capital cost required. In Figure 6.7(a), air enters at 0.01 m/s, adsorbing to q* over a day. In 6.7(b), air at speeds of 10 m/s saturates the sorbent with oxygen within 20 minutes.

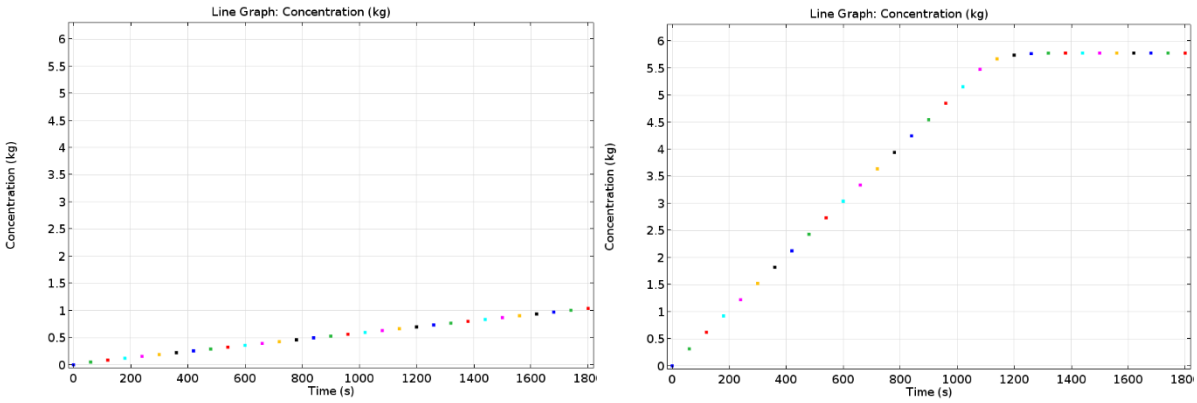

Figure 6.7.4: Adsorption behavior of oxygen at (a) 0.01 m/s on the left and (b) 10 m/s on the right. T = 500℃, air flow rate = 10 m/s, density = 5000 kg/m^3.

Notes on Studied Sensitivities

From Figure 6.7.1, it is clear that operating temperature has a significant impact on both sorbent capacity and kinetics. Temperature of the process is relatively easy to control, unlike material properties. Unfortunately, MIEC adsorption and desorption kinetics described by equations (6.1) and (6.4) are slower when operating at less than 500℃ in real life; the equations model the MIEC too simply. So, improved performance at 300℃ assumes improvements in MIEC behavior.

A breakthrough in MIEC preparation could make such a shift in adsorption and desorption coefficients possible. Such a change would yield an improvement in oxygen production rate by ~20%.

Increases in pressure are shown to improve the sorbent capacity and thus the amount of oxygen adsorbed per cycle, increasing the rate of oxygen production, however, the change is quite small (~10%) for the cost of compressing 130 tons+ of air per day by 8 atm.

Ultra-dense MIECs directly increase the rate of oxygen adsorption in simulation; however, real-life improvements may be less dramatic. We assume oxygen can diffuse quickly into the MIEC, but this may not be true for dense MIECs that carry high concentrations of oxygen.

7. Equipment List and Unit Descriptions

Adsorption Chamber

The adsorption chamber was designed to contain the adsorption and desorption tubes and maintain isothermal conditions. The chamber is stainless steel and contains the adsoption/desorption tubes and molten salt. The molten salt circulates throughout the chamber and acts as a heat transfer fluid (HTF) to transfer the heat from the exothermic adsorption to the endothermic desorption. The enthalpy of adsorption for the MIEC is -180 kJ/mol O_2. The enthalpy of desorption is +180 kJ/mol O_2.

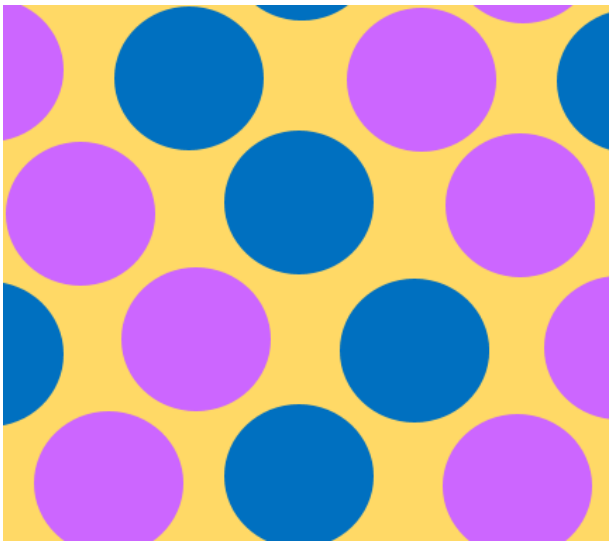

Figure 7.1.1: Diagram of the inside of the adsorption chamber. Each circle represents a tube that contains MIEC. Each tube switches between adsorption and desorption phases. The tubes that are currently adsorbing in the diagram are purple, while the tubes that are desorbing are blue. Surrounding the tubes is circulating solar salt in yellow which acts as a heat transfer medium to keep the system isothermal while the tubes in turn release heat during the adsorption phase and absorb heat during desorption phase.

Molten Salts was chosen as the HTF because they are cheaper, denser, and can retain more energy per volume than oil-based HTFs. The specific type of molten salt chosen is solar salt composed of 60% NaNO3, 40% KNO_3. Solar salt was chosen because it was the cheapest (0.49 $/kg) salt with the largest possible temperature range (220-600°C). More information about solar salt properties can be found in Appendix D: Solar Salt Properties.

Inlet Blower

The centrifugal blower is the first equipment into the process. The function of the blower was to compress inlet air from atmospheric pressure to 1.5 atm. The compression ratio was low enough to not require a compressor which is more expensive than a blower. An Electrical motor is used as driver. Mechanical efficiency was assumed to 75%, and the motor

efficiency was assumed to be 90%. In calculating bare module cost of the blower, material factor of 0.60 was used under the assumption that aluminum blades were used, and bare module factor 2.15 was used as recommended by Seider et al.

Vacuum

A jet ejector was used to form rough vacuum of 0.1 atm. To desorb oxygen from MIEC sorbents, pressure at or below 0.2 atm is needed. The function of the jet ejector was to desorb oxygen product and compress them into atmospheric pressure as a final product. The jet ejector was single stage. An electrical motor was used as a driver. Mechanical efficiency of 50% and bare-module factor of 2.15 were used as recommended by Seider et al.

Oxygen Heat Exchanger

The oxygen heat exchanger is a fixed head shell-and-tube heat exchanger used to heat the air stream S3 from 75.3℃ to 269℃ in parallel with the Waste Gas Heat Exchanger and to cool the outlet oxygen stream from the adsorber from 500℃ to 150℃. It was designed for the near maximum cooling of the oxygen stream. Air is in the shell side with the outlet oxygen from the adsorber in the tube side. The tubes are 3450 mm (11.3 ft) and made of stainless steel. The maximum pressure drop across the heat exchanger was set to 0.048atm as it is the lower limit of typical heat exchanger pressure drops (Mukherjee) and to avoid affecting the pressure in the rest of the process as much as possible. More information about the waste gas heat exchanger can be found in the specification sheets and EDR files can be found in Appendix C.

Waste Gas Heat Exchanger

The Waste Gas Heat Exchanger is a fixed head shell-and-tube heat exchanger used to heat the air stream S5 from 75.3℃ to 440℃ in parallel with the Oxygen Heat Exchanger. Air is in the shell side with the outlet waste gas from the adsorber in the tube side. The waste gas

is cooled from 50℃ to 150℃ before being released to the atmosphere. The tubes are 5700mm (18.7ft) and made of stainless steel. The maximum pressure drop across the shell side was set to 0.048atm as it is the lower limit of typical heat exchanger pressure drops(Mukherjee) and to avoid increasing the work of the vacuum. The maximum pressure drop across the tube side was set to 0.2atm so that the outlet of the waste gas to the atmosphere is slightly above atmospheric conditions of 1atm. More information about the waste gas heat exchanger can be found in the specification sheets and EDR files can be found in appendix C.

Furnace

A direct fired heater was used to heat the air stream before entering the adsorption chamber from 400℃ to 500℃. The heat duty is 156 kJ/s ($5.3*10^5$ BTU/hr). The bare module factor used to estimate the cost of the furnace was 1.86 corresponding to field fabricated direct fired heaters as opposed to shop fabricated.

8. Equipment Specification Sheets

Adsorption Chamber			
Item	Adsorption chamber		
Function	To contain the adsorption/desorption tubes and maintain isothermal conditions		
Operation	Continuous		
Performance of Unit			
	Inlet	Outlet	
Stream I.D.	S8	S9	500
Temperature (℃)	500	500	2.79
Mass Flow Rate (kg/s)	3.14	0.35	97.6
Mole Flow (mol/s)	108	10.8	1.19
Pressure (atm)	1.50	0.20	500
Phase	vapor	vapor	Vapor
Mechanical Design			
Material		Stainless steel	
		Solar Salt	
Diameter (m)		3	
Cost			
	Purchase Cost	$38,000	
	Solar Salt	$600	
	Total Bare Module Cost	**$115,000**	

Adsorption/Desorption Tubes	
Item	Adsorption/Desorption Tubes
No. Required	59
Function	To separate oxygen from air by adsorption
Mechanical Design	
Material	Stainless Steel
Tube length (m)	2
Tube radius (m)	0.125
Cross-sectional area (m^2)	0.196
Volume (m^3)	0.393
MIEC Catalyst	
Void fraction	0.4
Pellet porosity	0.5
Pellet volume (m^3)	0.157
MIEC Fill Volume (m^3)	0.079
Cost	
Purchase Cost	$10,000
Total Bare Module Cost	**$30,000**

Blower		
Item	Centrifugal Blower	
Function	To compress inlet air from 1 atm to 1.5 atm	
Operation	Continuous	
Performance of Unit		
	Inlet	Outlet
Stream I.D	S1	S2
Temperature (℃)	25	75.3
Mass Flow Rate (kg/s)	3.14	3.14
Mole Flow (mol/s)	108.3	108.3
Pressure (atm)	1.0	1.5
Phase	Vapor	Vapor
Mechanical Specifications		
Design Data	Material	Stainless steel
	Drive	Electric motor
	Power (hp)	270.7
	Mechanical efficiency	0.75
	Motor efficiency	0.9
Cost		
	Purchase cost	$49,000
	Total bare module cost	**$106,000**

Furnace		
Item	Direct Fired Heater	
Function	To heat the air stream up to 500℃ before entering the adsorption chamber	
Operation	Continuous	
Performance of Unit		
	Inlet	Outlet
Stream I.D	S7	S8
Temperature (℃)	400	500
Mass Flow Rate (kg/s)	3.14	3.14
Mole Flow (mol/s)	108	108
Pressure (atm)	1.50	1.50
Phase	vapor	vapor
Design Data		
Heat load (kW)	156	
Utilities	Natural Gas	
Cost		
	Purchase Cost	$56,000
	Total Bare Module Cost	**$105,000**

Oxygen Heat Exchanger				
Item	Shell-and-tube Heat Exchanger			
Function	To heat the inlet air stream from stream S3 from 75.3℃ to 269℃			
Operation	Continuous			
Performance of Unit				
	Shell Side: Air		Tube Side: Waste Gas	
	Inlet	Outlet	Inlet	Outlet
Stream I.D	S3	S4	S9	S10
Temperature (℃)	75.3	269	500	81.9
Mass Flow Rate (kg/s)	0.73	0.73	0.35	0.35
Mole Flow (mol/s)	25.3	25.3	10.8	10.8
Pressure (atm)	1.55	1.50	0.20	0.17
Phase	Vapor	Vapor	Vapor	Vapor
Design Data				
Max allowable pressure drop (atm)	Shell side	0.048	Tube side	0.048
Heat load (kW)	144			
Mechanical Specifications				
	Head Type		Fixed	
	Surface Area (m^2)		97.9	
	Material		Stainless steel	
Arrangement	Parallel		1	
	Series		2	
Tubes Specifications				
	Number		237	
	Length (m)		3.40	
	Passes		1	
	O.D. (mm)		19.05	
	Pitch (mm)		23.81	
	Pattern		30	
Cost				
	Material		$29,000	
	Total		**$65,000**	

Vacuum		
Item	Jet ejector	
Function	To compress inlet air from 0.1 atm to 1 atm	
Operation	Continuous	
Performance of Unit		
	Inlet	Outlet
Stream I.D	S10	S11
Temperature (℃)	80	403
Mass Flow Rate (kg/s)	0.35	0.35
Mole Flow (mol/s)	10.9	10.9
Pressure (atm)	0.1	1.0
Phase	Vapor	Vapor
Design Data		
	Material	Stainless steel
	Drive	Electric motor
	Power (hp)	238.1
	Mechanical efficiency	0.5
Cost		
	Purchase cost	$6,000
	Total bare module cost	**$13,000**

Waste Gas Heat Exchanger				
Item	Shell-and-tube Heat Exchanger			
Function	To heat the inlet air stream from stream S5 from 75.3℃ to 440℃			
Operation	Continuous			
Performance of Unit				
	Shell Side: Air		Tube Side: Waste Gas	
	Inlet	Outlet	Inlet	Outlet
Stream I.D	S5	S6	500	150
Temperature (℃)	75.3	440	500	150
Mass Flow Rate(kg/s)	2.41	2.41	2.79	2.79
Mole Flow (mol/s)	83.2	83.2	97.6	97.6
Pressure (atm)	1.55	1.50	1.19	1.18
Phase	Vapor	Vapor	Vapor	Vapor
Design Data				
Max allowable pressure drop (atm)	Shell side	0.048	Tube side	0.2
Heat load (kW)	907			
Mechanical Specifications				
	Head Type		Fixed	
	Surface Area(m^2)		485	
	Material		Stainless steel	
Arrangement	Parallel		3	
	Series		1	
Tubes Specifications				
	Number		480	
	Length (m)		5.7	
	Passes		1	
	O.D. (mm)		19.1	
	Pitch (mm)		23.8	
	Pattern		30	
Cost				
	Material		$93,000	
	Total		**$178,000**	

9. Profitability Analysis

9.1 Introduction

With the current market price of oxygen at $40 per ton, return on investment is -7.1%, and therefore producing oxygen using MIEC sorbents is not profitable. With a depreciation rate of 15%, and income tax of 37%, the net loss is $70,000 at the maximum production capacity of the process.

However, considering that MIECs are still a developing technology, there is the potential that it will be profitable in the future. A number of factors, including operating pressure, temperature, and desorption rate of MIECs drastically change the cost required to produce each ton of oxygen.

Further research into operating pressure, temperature, and desorption rate will make MIEC sorbents more competitive. The general economics of the process are shown in Figure 9.1.1, and will be presented in detail throughout the rest of the section. Also, it should be noted that unlike other design projects, because the technology of MIEC is still being developed, part of the goal of the project was to analyze various operating conditions and find the condition that gave the cheapest price per ton of oxygen. While the economic analysis of current MIECs proved unprofitable at $40/ton, we found that a selling price $56.70/ton would break even. Invention of the MIECs with a kinetic adsorption and desorption constant increased by a factor of 10 was also found to break even.

The Internal Rate of Return (IRR) for this project is	-28.08%
The Net Present Value (NPV) of this project in 2016 is	$ (990,300)

ROI Analysis (Third Production Year)

Annual Sales	**370,799**
Annual Costs	**(418,109)**
Depreciation	**(90,077)**
Income Tax	**50,833**
Net Earnings	**(86,554)**
Total Capital Investment	**1,169,294**
ROI	**-7.40%**

Figure 9.1.1: Profitability Analysis

9.2 Cost Summary

9.2.1 Material Costs

Because this process is separating oxygen from air, the only material going into this process was air. Although MIEC sorbents and molten salts are used in the process, these were considered as equipment cost, not material cost. As a result, because air does not require any cost, the material cost in the process was considered to be $0.

9.2.2 Utility Costs

The two sources of utility costs are electricity and natural gas. Electricity is used to run the centrifugal blower and vacuum. Natural gas is used in the furnace. The utility cost per ton of oxygen produced is presented in Table 9.2.1.

Table 9.2.1: Utility Costs per ton of oxygen

Utility	Unit	Required energy per ton O2	Cost per Unit [$/kwh]	Cost/ton O2 [$/ton]
Electricity	kWh	304	0.077	23.4
Natural Gas	kWh	121	0.014	1.70
			Total Utilities Cost	25.1

The unit cost of electricity and natural gas for industrial use in the Gulf Coast was sourced from the U.S Energy Information Administration. The table above clearly shows that unit cost of electricity is about five times more expensive than that of natural gas. Accordingly, minimizing the compression ratio and flow rate of the blower and vacuum, which run on electricity, was prioritized over minimizing the cost of natural gas for the furnace. Even with that goal in mind, electricity accounted for 93% of the utility cost of the selected plant design. Natural gas accounted for the other 7%.

9.2.3 Equipment Costs

The following is a table of bare-module costs of equipment in the process. The plant produces only 30 tons/day of oxygen, so equipment sizes are relatively small, thereby making the bare-module cost lower than other industrial plants, which usually spend several millions of dollars on equipment. It should be noted that MIEC sorbent was listed as equipment, although it was not visible in the process flowsheets. It should also be noted that Heat Exchanger 1 is the bigger heat exchanger for cooling nitrogen outlet, and Heat Exchanger 2 is the smaller heat exchanger for cooling the oxygen product.

Table 9.2.2: Equipment Bare Module Cost

Equipment	Type	Bare-module cost
Centrifugal Blower	Process Machinery	$106,000
Jet Ejector	Process Machinery	$13,000
Furnace	Fabricated Equipment	$105,000
Adsorption Chamber	Fabricated Equipment	$115,000
Heat Exchanger 1	Fabricated Equipment	$178,000
Heat Exchanger 2	Fabricated Equipment	$65,000
Tubes	Fabricated Equipment	$30,000
MIEC Sorbents	Compound in System	$162,000
Solar Salt	Compound in System	$600
Total bare module cost:		$744,600

According to Table 9.2.2, the MIEC sorbent, adsorption chamber, centrifugal blower, furnace, and Heat Exchanger 1 cost over $100,000. Heat Exchanger 1, the adsorption chamber, the centrifugal blower, and the furnace are large compared to the other equipment. Those pieces of equipment are intake 270 tons/day of air, a higher flow rate than the other

equipment. Because of the high flow rate, the equipment has to be larger and is therefore more expensive. Heat Exchanger 2, on the other hand, is relatively small since its hot stream is of oxygen, which is approximately 21% the original inlet flowrate. The cost the MIEC sorbent was calculated by assuming a unit cost of $40/kg. The mass of MIEC sorbent needed to obtain 30 tons/day of oxygen is explained in Section 6.6, Mass of MIEC Required.

9.3 Investment Summary

The variable cost, working capital, fixed costs, and investment summaries were estimated based on literature called 'profitability analysis' provided by Seider et al. The following table presents the variable cost at 100% capacity of the plant. As mentioned earlier, because only raw material for the process is air, and therefore the material cost was assumed to be $0. The only byproduct from the system is nitrogen, so the byproduct price was also assumed to be $0.

Variable Costs at 100% Capacity:			
General Expenses			
Selling / Transfer Expenses:		$	11,880
Direct Research:		$	19,008
Allocated Research:		$	1,980
Administrative Expense:		$	7,920
Management Incentive Compensation:		$	4,950
Total General Expenses		$	45,738
Raw Materials	$0.000000 per tons of O2		$0
Byproducts	$0.000000 per tons of O2		$0
Utilities	$25.102000 per tons of O2		$248,510
Total Variable Costs		**$**	**294,248**

Figure 9.3.1: Annual Variable Costs

9.3.1 Fixed costs

Observation of fixed cost clearly shows that operation cost is relatively small compared to purchase cost of equipment. This plant assumed that there are no direct labors within the plant, which is how VPSA plants are run to produce oxygen. As a result, no cost was spent for wages, and returned a low cost for total fixed costs.

Operations			
	Direct Wages and Benefits	$	-
	Direct Salaries and Benefits	$	-
	Operating Supplies and Services	$	-
	Technical Assistance to Manufacturing	$	-
	Control Laboratory	$	-
	Total Operations	**$**	**-**
Maintenance			
	Wages and Benefits	$	45,239
	Salaries and Benefits	$	11,310
	Materials and Services	$	45,239
	Maintenance Overhead	$	2,262
	Total Maintenance	**$**	**104,050**
Operating Overhead			
	General Plant Overhead:	$	4,015
	Mechanical Department Services:	$	1,357
	Employee Relations Department:	$	3,336
	Business Services:	$	4,185
	Total Operating Overhead	**$**	**12,893**
Property Taxes and Insurance			
	Property Taxes and Insurance:	$	20,106
Other Annual Expenses			
	Rental Fees (Office and Laboratory Space):	$	-
	Licensing Fees:	$	-
	Miscellaneous:	$	-
	Total Other Annual Expenses	**$**	**-**
Total Fixed Costs		**$**	**137,050**

Figure 9.3.2: Fixed Costs Summary

9.3.2 Total Permanent Investment

The total bare module cost for the equipment is approximately $700,000. The cost of site preparation and service facilities were estimated as 5% of the total bare module cost. Cost of contingencies and contractor fees, cost of land, and cost of plant start up were estimated as 18% of direct permanent investment, 2% and 10% of total depreciable capital each. The site was specified to operate on the U.S Gulf Coast where many industrial customers in need of oxygen solutions exist. Accordingly, the site factor was assumed to be 1.

Total Bare Module Costs:			
Fabricated Equipment	$	505,662	
Process Machinery	$	106,124	
Spares	$	-	
Storage	$	-	
Other Equipment	$	162,728	
Catalysts	$	-	
Computers, Software, Etc.	$	-	
Total Bare Module Costs:			**$ 774,514**
Direct Permanent Investment			
Cost of Site Preparations:	$	38,726	
Cost of Service Facilities:	$	38,726	
Allocated Costs for utility plants and related facilities:	$	-	
Direct Permanent Investment			**$ 851,965**
Total Depreciable Capital			
Cost of Contingencies & Contractor Fees	$	153,354	
Total Depreciable Capital			**$ 1,005,319**
Total Permanent Investment			
Cost of Land:	$	20,106	
Cost of Royalties:	$	-	
Cost of Plant Start-Up:	$	100,532	
Total Permanent Investment - Unadjusted			$ 1,125,957
Site Factor			1.00
Total Permanent Investment			**$ 1,125,957**

Figure 9.3.1: Investment Summary

9.3.3 Working Capital

The working capital was calculated 30 days calculation for accounts receivable, cash reserve, and accounts payable. In addition, 4 days were used for oxygen inventory, and 2 days were used for raw materials. The working capitals in present value were added to total permanent investment to obtain total capital investment of approximately 1.3 million dollars.

	2019	2020	2021
Accounts Receivable	$ 14,647	$ 7,323	$ 7,323
Cash Reserves	$ 14,260	$ 7,130	$ 7,130
Accounts Payable	$ (9,191)	$ (4,596)	$ (4,596)
O2 Inventory	$ 1,953	$ 976	$ 976
Raw Materials	$ -	$ -	$ -
Total	**$ 21,668**	**$ 10,834**	**$ 10,834**
Present Value at 15%	*$ 14,247*	*$ 6,194*	*$ 5,387*

Total Capital Investment **$ 1,151,785**

Figure 9.3.2: Working Capital Summary

9.4 Cash Flow and Cost Sensitivity Analysis

Through cash flow analysis, the initial capital cost, the year of positive cash flow, and the net present value of the project can be found. In this case, the process is actually losing money for each ton of oxygen sold. Again, this is due to the fact that MIEC sorbents are still under development and that part of the project was about determining the ideal operating condition to make the price per ton of oxygen lowest, rather than making profit from the technology immediately. The cash flow analysis used a 10-year modified accelerated cost system recovery system (MACRS) depreciation schedule. As figure 9.4.1 shows, no revenue is produced, and the final net present value (NPV) is approximately negative 0.9 million dollars.

Cost Sensitivity Analysis was performed to observe project's sensitivity towards variety of changes in cost, such as product price, variable costs, fixed costs, and total permanent investment. Product price and other costs were varied up to 50%, and change in

the internal rate of return (IRR) was observed. Tables below show that the project was most sensitive to product price and variable cost. However, the product price for oxygen is already set due to other competing technology such as VPSA. So in order to make the technology of MIEC more competitive, more effort should be put in to reduce the variable cost. Most of the variable cost in the project is from the utility cost, which as mentioned before, is mostly the electricity cost to run two compression processes. With current status of MIEC sorbents, in order for the sorbents to adsorb air, the operating temperature must be 500℃ or higher, which makes product oxygen to be hot. This makes the volumetric flow rate of air very high and put more work load on the jet ejector at the end of the process. If the operating temperature of MIEC could be reduced with further research, the sorbent will be more competitive in the future.

Sales	Capital Costs	Working Capital	Var Costs	Fixed Costs	Depreciation	Depletion Allowance	Taxible Income	Taxes	Net Earnings	Cash Flow	Cumulative Net Present Value at 15%
-	-	-	-	-	-	-	-	-	-	-	-
-	(1,126,000)	-	-	-	-	-	-	-	-	(1,126,000)	(979,100)
-	-	-	-	-	-	-	-	-	-	-	(979,100)
-	-	(21,700)	-	-	-	-	-	-	-	(21,700)	(993,300)
178,200	-	(10,800)	(132,400)	(137,100)	(100,500)	-	(191,800)	71,000	(120,800)	(31,100)	(1,011,100)
272,600	-	(10,800)	(202,600)	(139,800)	(181,000)	-	(250,700)	92,800	(157,900)	12,200	(1,005,100)
370,800	-	-	(275,500)	(142,600)	(144,800)	-	(192,100)	71,100	(121,000)	23,800	(994,800)
378,200	-	-	(281,000)	(145,400)	(115,800)	-	(164,100)	60,700	(103,400)	12,400	(990,100)
385,800	-	-	(286,700)	(148,300)	(92,700)	-	(141,900)	52,500	(89,400)	3,300	(989,100)
393,500	-	-	(292,400)	(151,300)	(74,100)	-	(124,300)	46,000	(78,300)	(4,200)	(990,300)
401,400	-	-	(298,200)	(154,300)	(65,800)	-	(117,100)	43,300	(73,700)	(7,900)	(992,200)
409,400	-	-	(304,200)	(157,400)	(65,800)	-	(118,100)	43,700	(74,400)	(8,500)	(994,000)
417,600	-	-	(310,300)	(160,600)	(65,900)	-	(119,200)	44,100	(75,100)	(9,200)	(995,800)
425,900	-	43,300	(316,500)	(163,800)	(65,800)	-	(120,200)	44,500	(75,700)	33,500	(990,300)

Figure 9.4.1: Process Cash Flow

Product Price	Variable Costs										
	$147,124	$176,549	$205,973	$235,398	$264,823	***$294,248***	$323,673	$353,097	$382,522	$411,947	$441,372
$20.00	Negative IRR	Negative IRR	Negative IRR	Negative IRR	Negative IRR	Negative IRR	Negative IRR	Negative IRR	Negative IRR	Negative IRR	Negative IRR
$24.00	Negative IRR	Negative IRR	Negative IRR	Negative IRR	Negative IRR	Negative IRR	Negative IRR	Negative IRR	Negative IRR	Negative IRR	Negative IRR
$28.00	-18.63%	Negative IRR	Negative IRR	Negative IRR	Negative IRR	Negative IRR	Negative IRR	Negative IRR	Negative IRR	Negative IRR	Negative IRR
$32.00	-11.28%	-16.14%	-24.69%	Negative IRR	Negative IRR	Negative IRR	Negative IRR	Negative IRR	Negative IRR	Negative IRR	Negative IRR
$36.00	-6.70%	-9.90%	-14.12%	-20.64%	Negative IRR	Negative IRR	Negative IRR	Negative IRR	Negative IRR	Negative IRR	Negative IRR
$40.00	-3.27%	-5.72%	-8.66%	-12.41%	-17.76%	-28.08%	Negative IRR	Negative IRR	Negative IRR	Negative IRR	Negative IRR
$44.00	-0.48%	-2.50%	-4.81%	-7.54%	-10.93%	-15.50%	-22.97%	Negative IRR	Negative IRR	Negative IRR	Negative IRR
$48.00	1.89%	0.16%	-1.77%	-3.96%	-6.51%	-9.60%	-13.62%	-19.57%	Negative IRR	Negative IRR	Negative IRR
$52.00	3.97%	2.44%	0.77%	-1.07%	-3.15%	-5.55%	-8.41%	-12.01%	-17.00%	-25.70%	Negative IRR
$56.00	5.82%	4.45%	2.98%	1.36%	-0.41%	-2.40%	-4.66%	-7.32%	-10.59%	-14.92%	-21.60%
$60.00	7.51%	6.26%	4.93%	3.49%	1.93%	0.22%	-1.68%	-3.83%	-6.32%	-9.33%	-13.16%

Figure 9.4.2: Sensitivity Analysis on IRR of Variable Cost vs Product Price

Product Price \ Fixed Costs	$68,525	$82,230	$95,935	$109,640	$123,345	***$137,050***	$150,755	$164,460	$178,165	$191,870	$205,575
$20.00	Negative IRR	Negative IRR	Negative IRR	Negative IRR	Negative IRR	Negative IRR	Negative IRR	Negative IRR	Negative IRR	Negative IRR	Negative IRR
$24.00	Negative IRR	Negative IRR	Negative IRR	Negative IRR	Negative IRR	Negative IRR	Negative IRR	Negative IRR	Negative IRR	Negative IRR	Negative IRR
$28.00	Negative IRR	Negative IRR	Negative IRR	Negative IRR	Negative IRR	Negative IRR	Negative IRR	Negative IRR	Negative IRR	Negative IRR	Negative IRR
$32.00	Negative IRR	Negative IRR	Negative IRR	Negative IRR	Negative IRR	Negative IRR	Negative IRR	Negative IRR	Negative IRR	Negative IRR	Negative IRR
$36.00	-15.93%	-19.66%	-25.23%	Negative IRR	Negative IRR	Negative IRR	Negative IRR	Negative IRR	Negative IRR	Negative IRR	Negative IRR
$40.00	-9.67%	-11.77%	-14.26%	-17.35%	-21.50%	-28.08%	Negative IRR	Negative IRR	Negative IRR	Negative IRR	Negative IRR
$44.00	-5.49%	-7.02%	-8.71%	-10.63%	-12.84%	-15.50%	-18.86%	-23.53%	Negative IRR	Negative IRR	Negative IRR
$48.00	-2.27%	-3.49%	-4.82%	-6.26%	-7.84%	-9.60%	-11.61%	-13.96%	-16.81%	-20.49%	-25.81%
$52.00	0.39%	-0.65%	-1.75%	-2.93%	-4.19%	-5.55%	-7.04%	-8.68%	-10.52%	-12.63%	-15.12%
$56.00	2.67%	1.76%	0.80%	-0.20%	-1.27%	-2.40%	-3.60%	-4.90%	-6.30%	-7.84%	-9.54%
$60.00	4.68%	3.86%	3.01%	2.13%	1.20%	0.22%	-0.80%	-1.89%	-3.04%	-4.28%	-5.61%

Figure 9.4.3 : Sensitivity Analysis on IRR of Fixed Cost vs Product Price

Product Price \ Total Permanent Investment	$562,978	$675,574	$788,170	$900,765	$1,013,361	***$1,125,957***	$1,238,552	$1,351,148	$1,463,744	$1,576,340	$1,688,935
$20.00	Negative IRR	Negative IRR	Negative IRR	Negative IRR	Negative IRR	Negative IRR	Negative IRR	Negative IRR	Negative IRR	Negative IRR	Negative IRR
$24.00	Negative IRR	Negative IRR	Negative IRR	Negative IRR	Negative IRR	Negative IRR	Negative IRR	Negative IRR	Negative IRR	Negative IRR	Negative IRR
$28.00	Negative IRR	Negative IRR	Negative IRR	Negative IRR	Negative IRR	Negative IRR	Negative IRR	Negative IRR	Negative IRR	Negative IRR	Negative IRR
$32.00	Negative IRR	Negative IRR	Negative IRR	Negative IRR	Negative IRR	Negative IRR	Negative IRR	Negative IRR	Negative IRR	Negative IRR	Negative IRR
$36.00	-12.22%	-20.95%	Negative IRR	Negative IRR	Negative IRR	Negative IRR	Negative IRR	Negative IRR	Negative IRR	Negative IRR	Negative IRR
$40.00	0.54%	-5.69%	-11.17%	-16.36%	-21.74%	-28.08%	Negative IRR	Negative IRR	Negative IRR	Negative IRR	Negative IRR
$44.00	7.76%	1.64%	-3.42%	-7.80%	-11.76%	-15.50%	-19.18%	-23.00%	-27.28%	Negative IRR	Negative IRR
$48.00	13.05%	6.77%	1.71%	-2.55%	-6.27%	-9.60%	-12.68%	-15.60%	-18.43%	-21.27%	-24.21%
$52.00	17.32%	10.81%	5.64%	1.36%	-2.32%	-5.55%	-8.46%	-11.14%	-13.64%	-16.02%	-18.33%
$56.00	20.94%	14.21%	8.90%	4.53%	0.83%	-2.40%	-5.26%	-7.85%	-10.24%	-12.46%	-14.55%
$60.00	24.13%	17.15%	11.69%	7.23%	3.47%	0.22%	-2.64%	-5.21%	-7.55%	-9.70%	-11.71%

Figure 9.4.4 : Sensitivity Analysis on IRR of Total Permanent Investment vs Product Price

9.5 Operating Condition Sensitivity Analysis

Sensitivity analysis was done by varying three factors within the system. Inlet temperature, pressure, and air flow velocity into the adsorption chamber was varied to obtain total production cost per ton of oxygen. The maintenance cost and operation cost was not taken into account for this analysis. The analysis for adsorber inlet temperature of 500℃ is shown in the following table.

Table 9.3 Change in cost of equipment based on change of operating

Inlet temperature (℃)	Inlet pressure (atm)	Inlet air flow velocity (m/s)	MIEC cost ($/tonO2)	Adsorber cost ($/tonO2)	Blower+ejector cost ($/tonO2)	Heat exchangers + Furnace cost($/tonO2)	Production cost ($/tonO2)
500	1.25	0.32	$17.10	$6.66	$24.46	$8.63	$56.86
500	1.25	1.00	$5.25	$2.85	$24.19	$8.63	$40.92
500	1.25	3.16	$2.17	$1.71	$26.90	$8.63	$39.41
500	1.25	10.00	$1.17	$1.28	$35.02	$8.63	$46.10
500	1.5	0.32	$13.88	$5.66	$29.62	$7.69	$56.84
500	1.5	1.00	$4.44	$2.59	$29.79	$7.69	$44.51
500	1.5	3.16	$1.64	$1.47	$32.18	$5.23	$40.51
500	1.5	10.00	$0.89	$1.14	$44.16	$5.23	$51.42
500	2	0.32	$10.44	$4.57	$38.82	$5.80	$59.63
500	2	1.00	$3.39	$2.19	$39.42	$5.80	$50.80
500	2	3.16	$1.39	$1.37	$46.51	$5.80	$55.08
500	2	10.00	$0.89	$1.14	$78.14	$5.80	$85.97
500	3	0.32	$6.58	$3.32	$51.11	$6.72	$67.73
500	3	1.00	$2.36	$1.79	$55.87	$6.72	$66.75
500	3	3.16	$1.11	$1.23	$75.50	$6.72	$84.56
500	3	10.00	$0.61	$0.95	$119.55	$6.72	$127.84

It should be noted that the table above shows only portion of the sensitivity analysis. The entire sensitivity analysis table was too big, so the portion that was most relevant in selecting the

most cost effective operating condition under was presented. The complete table of operating conditions analysis is shown in the Appendix E.

Inlet air velocity accounts for different mass flow rates into the adsorption chamber. Inlet temperature, pressure, and air velocity have different effects on different equipment. As shown in table above, higher pressure increases power consumption of blower, but increases adsorption rate of MIEC. Increasing air velocity increases work load of furnace and blower, but decreases number of tubes needed within the column, thereby decreasing the cost of column. And as shown in the complete table from appendix, higher temperature increases power consumption of the furnace and blower, but, at the same time, increases the efficiency of adsorption of MIEC, thereby lowering the price of MIEC and adsorbion chamber. Because all three factors affects the cost in various ways, three different temperature, three different pressure, and six different air flow velocity was selected for sensitivity analysis to find the ideal operating condition that would give the cheapest oxygen production cost.

According to studies done regarding MIECs so far, MIEC sorbents functions at a temperature of 500℃ or above. Therefore, in doing profitability analysis, the operating conditions that had temperature of 500℃ or above were considered for selecting operating conditions. Among various conditions the two conditions that returned lowest production costs gave $39.41 and $40.51 per ton oxygen. Among the two, the second option was selected as our operation condition, because the condition had a low capital cost and high utility cost. By selecting the second condition, the plant would have low initial investment and may lower the production cost if the plant is built on location where the electricity cost is even cheaper. Therefore, the operating condition that had temperature of 500℃, pressure of 1.5 atm, and inlet velocity of 3.16 m/s was selected as operating condition for this project.

As mentioned in the beginning of the section, the return on investment was about negative 7.4%. Part of this project was also finding the operation condition to find the break even point. There were two ways to find the break even point. One was changing the oxygen selling price for the operating condition that was selected above. Again using the literature provided by Seider et al, it was found that under the current operating condition, selling price of $56.70 per ton of oxygen is needed to reach the break even point. Another way to reach the break even point was tuning kinetic constant for adsorption (k_{ads}) and the loading capacity (q*), while keeping the operating conditions as above. The kinetic constant was changed from $2x10^{-2}$ s^{-1} to $2x10^{-1}$ s^{-1}, and the loading capacity was changed to 6500kg/m^3 from 3500kg/m^3, With such change in kinetic constant and loading capacity, it was found that temperature of 500℃, inlet pressure of 1.25atm, and inlet velocity of 10m/s returns break even point. To be exact, ROI was 0.2%, which is slightly higher than break even point, but that condition was the closest to break even point under the conditions that we tested. Profitability analysis regarding both cases are presented in Appendix F.

10. Conclusions and Recommendations

10.1 Recommendations and Prospects for Future Work

The utility cost running the vacuum is the most expensive part in the process, so further steps may be taken to reduce the utility cost of the vacuum or design the process without it. To reduce the cost of the vacuum, a fourth heat exchanger could be placed after the oxygen heat exchanger to cool the oxygen stream down to 25℃ or lower. This would decrease the volumetric flow rate of the oxygen stream, decreasing the necessary size and cost of the vacuum.

Furthermore, as it was shown in the sensitivity analysis, production cost of oxygen varies significantly depending on operating conditions. The sensitivity analysis done in the report showed that increasing the adsorption kinetic constant by a factor of ten and loading capacity by a factor of two enabled the process to reach break even point. Therefore, further research of MIEC to reach such increase in those values will make MIEC more competitive.

Also, further improvement will be needed for desorption pressure. At current stage, pressure lower than 0.2 atm is needed to desorb oxygen from MIEC sorbents. The utility cost over 10 years of operation is makes up a significant portion of entire production cost of oxygen. However, if the improvement in the technology allows desorption pressure to be higher than now, the utility cost for the vacuum system will decrease, which can possibly make MIEC sorbents more competitive.

10.2 Conclusion

Our team decided to evaluate the potential if MIEC technology when incorporated into a VPSA system with an output of 30 tons per day of 99.99% pure oxygen for a number of reasons. In order to accurately understand the potential of this technology in the market we decided it would be most useful to select output specifications that match those of current VPSA systems in the market. The figure of 30 ton/day was selected because it fell within the range of most commercial systems, and it was also an output that can be marketed to a number of industries.

Despite our system being designed with commercial zeolite VPSA system in mind, there are major distinctions. The most salient deviation from the zeolite systems is the fact that our system needs to operate at 500C versus room temperature. This operating conditions results in our system requiring a heat exchanger network as well as a gas furnace. Our system also makes the assumption that the columns are isothermal, which requires them to be contained in a molten solar salt bath, to facilitate heat transfer across the adsorption and desorption columns. Another major difference between the conventional zeolite systems is the number and size of the adsorption/desorption columns in our system. Where most zeolite based systems operate with two distinct packed columns, our system requires 60 smaller packed adsorption/desorption tubes which are staggered to produce a constant product stream.

30 tons/day of high-purity oxygen is produced by using a centrifugal blower to increase the pressure of air up to 1.5 atm, then using two shell-and-tube heat exchangers and a furnace to increase the temperature of air from 25℃ to 500℃. The air then an adsorption chamber in which oxygen in turn adsorbs and desorbs on MIEC to produce high-purity oxygen. The oxygen desorbs due to a pressure decrease to below 0.2atm caused by a jet ejector vacuum.

11. Acknowledgements

We would like to thank Dr. Matthew Targett for conceptualizing this project and mentoring us throughout the project. We would also like to thank Dr. Talid Sinno and Professor Leonard Fabiano for their support and engagement in this project. Finally, we would like to thank the industrial consultants, Mr. Adam A. Brostow, Mr. Stephen M. Tieri and Mr. Vrana Vrana, who offered their expertise in weekly design meetings and email correspondences.

12. References

Ansys. “Fluent.” 2016. Web. http://www.ansys.com/Products/Fluids/ANSYS-Fluent

Ashcraft.B, Jennifer Swenton, 99% Oxygen Production with Zeolites and Pressure Swing Adsorption: Designs and Economic Analysis, *Chemical and Biological Materials, University of Oklahoma,* 2007

Chart Industries, AirSep ASV Series Tonnage Plants, 2016

Chiang, Anthony S.t. "An Analytical Solution to Equilibrium PSA Cycles." *Chemical Engineering Science* 51.2 (1996): 207-16. Web.

“Commodities: Latest Natural Gas Price & Chart.” NASDAQ.com. Web. 11 Apr. 2016. <http://www.nasdaq.com/markets/natural-gas.aspx?timeframe=10y>.

Ecija. Ana, Karmele Vidal, Aitor Larrañaga, Luis Ortega-San-Martín and María Isabel Arriortua (2012). Synthetic Methods for Perovskite Materials; Structure and Morphology, Advances in Crystallization Processes, Dr. Yitzhak Mastai (Ed.), ISBN: 978-953-51-0581-7, InTech

Ellett, Anna Judith. *Oxygen Permeation and Thermo-Chemical Stability of Oxygen Separation Membrane Materials for the Oxyfuel Process*. Jülich: Forschungszentrum, Zentralbibliothek, 2009. Print.

Grande, Carlos A. "Advances in Pressure Swing Adsorption for Gas Separation." *ISRN Chemical Engineering* 2012 (2012): 1-13. Web.

Green, Don and Robert Perry. *Perry's Chemical Engineers' Handbook (6 ed.).* MCGraw-Hill. 1984. ISBN 0-07-049479-7. Page 3-162.

He, Yufeng, Xuefeng Zhu, Qiming Li, and Weishen Yang. "Perovskite Oxide Absorbents for Oxygen Separation." *AIChE Journal AIChE J.* 55.12 (2009): 3125-133. Web.

HighBeam Business, Industrial Gases**,** *NAICS 325120: Industrial Gas Manufacturing,* Farmington Hills, Michigan *2016.*

Hutson. N.D,† Barbara A. Reisner,‡ Ralph T. Yang,*,† and Brian H. Toby‡ , Silver Ion-Exchanged Zeolites Y, X, and Low-Silica X: Observations of Thermally Induced Cation/Cluster Migration and the Resulting Effects on the Equilibrium Adsorption of Nitrogen, *Department of Chemical Engineering, University of Michigan, Ann Arbor, Michigan 48109, and Center for Neutron Research, National Institute of Standards and Technology, Gaithersburg, Maryland 20899-8562* Received April 8, 2000. Revised Manuscript Received July 13, 2000.

Hyoungjeen Jeen , Woo Seok Choi , John W. Freeland , Hiromichi Ohta , Chang Uk Jung, and Ho Nyung Lee, *Topotactic phase transformation of the brownmillerite SrCoO2.5 to the perovskite SrCoO3-δ*.

Incropera, Frank, DeWitt, David, Bergman, Theodore, and Lavine, Adrienne. *Fundamentals of Heat and Mass Transfer. 7ed. Wiley.* (2011).

Kearney, D., U. Herrmann, P. Nava, B. Kelly, R. Mahoney, J. Pacheco, R. Cable, N. Potrovitza, D. Blake, and H. Price. "Evaluation of a Molten Salt Heat Transfer Fluid in a Parabolic Trough Solar Field." *Solar Energy* (2002). Web.

Kelly, S,M. , Director OTM R&D, Praxair's Oxygen Transport Membranes for Oxycombustion and Syngas Applications NT43088, August 1st, 2014. Web.

Kim, Dong Hyun. "Linear Driving Force Formulas for Diffusion and Reaction in Porous Catalysts." *AIChE Journal AIChE J.* 35.2 (1989): 343-46. Web.

Lemes-Rachadel, Priscila, Giulliani Sachinelli Garcia, Ricardo Antonio Francisco Machado, Dachamir Hotza, and João Carlos Diniz Da Costa. "Current Developments of Mixed Conducting Membranes on Porous Substrates." *Mat. Res. Materials Research* 17.1 (2014): 242-49. Web.

Linde AG, Oxygen generation. By Vacuum Pressure Swing Adsorption, *Engineering Division*, Dr.-Carl-von-Linde-Strasse 6–14, 82049 Pullach, Germany.

Liu, Meilin. "Equivalent Circuit Approximation to Porous Mixed-Conducting Oxygen Electrodes in Solid-State Cells." *Journal of The Electrochemical Society J. Electrochem. Soc.* 145.1 (1998): 142. Web.

Mofarahi, Masoud, Jafar Towfighi, and Leila Fathi. "Oxygen Separation from Air by Four-Bed Pressure Swing Adsorption." *Industrial & Engineering Chemistry Research Ind. Eng. Chem. Res.* 48.11 (2009): 5439-444. Web.

Morea. S, Oxygen & Hydrogen Gas Manufacturing in the US, *IBISWorld Industry Report 32512*, July 2015.

Praxair Technology, Inc., VPSA OXYGEN GAS PRODUCTION, 2013-2016

Rao. P, Muller. M, Industrial Oxygen: Its Generation and Use, *Center for Advanced Energy Systems*, Rutgers, the State University of New Jersey, 2007.

Rodrigues, Alirio, and Peter Lewis Silveston. "Pressure and Temperature Swing Reactors." *Periodic Operation of Chemical Reactors* (2013): 637-77. Web.

Sircar, S., and J. R. Hufton. "Intraparticle Adsorbate Concentration Profile for Linear Driving Force Model." *AIChE Journal AIChE J.* 46.3 (2000): 659-60. Web.

Sirman.J , B.A. vanHassel, L. Switzer, G.M. Christie**,** A Comparison of Oxygen Supply Systems for Combustion Applications *Fourth Annual Conference on Carbon Capture & Sequestration* May 2-5, 2005.

SU2. "SU2 The Open-Source CFD Code." Web. 2016. http://su2.stanford.edu/

Sunarso, J., S. Baumann, J.m. Serra, W.a. Meulenberg, S. Liu, Y.s. Lin, and J.c. Diniz Da Costa. "Mixed Ionic–electronic Conducting (MIEC) Ceramic-based Membranes for Oxygen Separation." *Journal of Membrane Science* 320.1-2 (2008): 13-41. Web.

Yang, R. T. *Adsorbents: Fundamentals and Applications*. Hoboken, NJ: Wiley-Interscience, 2003. Print.

13. Appendix

Appendix A: Sample Calculations

A.1 Total Cost of Heating

Equations used to calculate the cost of the furnace are shown in appendix B.

T=440℃

T_{O2HX}= 268.64℃

T*=500℃

P*=1.25 atm absolute

Furnace Heat Duty calculated by Aspen plus = 532216.3375 BTU/hr

Cost of the waste gas heat exchanger, calculated by Aspen EDR = $177,696

Cost of the oxygen heat exchanger, calculated by Aspen EDR = $64,670

mass fraction of air stream sent to the oxygen heat exchanger = 0.233

mass fraction of air stream sent to the waste gas heat exchanger = 0.766

T_m = 0.233*268.64+0.766*440=399.6℃

C_B= exp{[0.32325+0.76[ln(532216.3375)]}=33617.79728

C_p= 0.986*1.7*33617.79728=56350.1518

C=56350.1518*1.86= $104,811.2823

Natural gas cost:

$$4 * 10^{-6} \frac{\$}{\text{BTU}} \times 532216 \frac{\text{BTU}}{\text{hr}} \times 10\text{yr} \times \frac{330\text{days}}{\text{yr}} \times \frac{24\text{hr}}{\text{day}} = \$168{,}606 \frac{\text{gas}}{10\text{yrs}}$$

Total Cost of Heating = $104,811.28+$168,606+$177,696+$64,670=$515,783

A.2 Bare Module Cost Calculation

Bare module cost of centrifugal blower :

$$C_B = \exp\{6.8929 + 0.7900[ln(P_c)]\}$$

$$C_{BM} = F_{BM}\, F_M\, C_B$$

C_{BM} = Bare module cost
C_B = Base cost
P_C = Power consumption (hp)
F_{BM} = Bare module factor
F_M = Material factor

Sample calculation :

$$C_B = \exp\{6.8929 + 0.7900[ln(270.7)]\} = \$82265$$

$$C_{BM} = (2.15)(0.6)(\$82265) = \$106{,}122$$

Jet ejector:

$$S = \frac{M}{P_I}$$

$$C_P = 1690 * S^{0.41}$$

$$C_{BM} = F_{BM} C_P$$

C_{BM} = Bare module cost
C_P = Purchase cost
F_{BM} = Bare module factor
S = size factor (lb/hr-torr)
M =mass flow rate (lb/hr)
P_I =Inlet pressure (torr)

Sample Calculation:

$$S = \frac{\left(\frac{30\text{ton}}{\text{day}}\right)\left(\frac{1000\text{kg}}{\text{ton}}\right)\left(\frac{2.205\text{lb}}{\text{kg}}\right)\left(\frac{\text{day}}{24\text{hr}}\right)}{0.15\text{atm}\left(\frac{760\text{torr}}{\text{atm}}\right)} = \frac{24.2\text{lb}}{\text{hr torr}}$$

$$C_P = 1690(24.2)^{0.41} = \$6238$$

$$C_{BM} = (2.15)(\$6238) = \$13{,}411$$

Adsorption chamber:

$$C_V = \exp\{8.9552 - 0.2330[\ln(W)] + 0.04333[\ln(W)]^2\}$$

$$W = \pi(D_i + t_s)(L + 0.8D_i)t_s\rho$$

$$C_{PL} = 2005(D_i)^{0.20294}$$

$$C_{BM} = F_{BM}(F_M C_V + C_{PL})$$

C_{BM} = Bare module cost
C_V = Vessel cost
C_{PL} = Platform and ladder cost
W = weight (lb)
D_i = Inner diameter of the vessel (ft)
L = Length of the vessel (ft)
t_s = shell thickness (ft)
F_{BM} = Bare module factor

Sample calculation:

$$W = \pi\left(9\text{ft} + \left(\frac{1}{4}\text{in}\right)\left(\frac{\text{ft}}{12\text{in}}\right)\right)\left(6.56\text{ft} + 0.8(9\text{ft})\right)\left(\frac{1}{4}\text{in}\right)\left(\frac{\text{ft}}{12\text{in}}\right)\left(\frac{499.39\text{lb}}{\text{ft}^3}\right) = 4057\text{lb}$$

$$C_V = \exp\{8.9552 - 0.2330[\ln(4057)] + 0.04333[\ln(4057)]^2\} = \$22254$$

$$C_{BM} = (3.05)\big((1.7)(22254)\big) = \$115{,}397$$

Tubes:

$$\mathrm{W} = \frac{\pi}{4}[(D_i + 2t_s)^2 - (D_i)^2](\mathrm{L})(n)\rho$$

$$\mathrm{C_{BM}} = \mathrm{F_{BM}F_M W} = \$29{,}682$$

D_i=inner diameter of tube (ft)
T_s =thickness of tube (ft)
L=length of tubes (ft)
N= number of tubes
ρ =density of material of tube (lb/ft)

Sample Calculation

$$\mathrm{W} = \frac{\pi}{4}\left[\left(0.82\mathrm{ft} + \left(\frac{2}{48}\mathrm{ft}\right)\right)^2 - (0.82\mathrm{ft})^2\right](6.56\mathrm{ft})(59\mathrm{tubes})\left(\frac{499.39\mathrm{lb}}{\mathrm{ft}^3}\right) = 3244\mathrm{lb}$$

$$C_{BM} = (3.05)(3)(3244\mathrm{lb}) = \$29{,}682$$

Adding the two costs of vessel and tubes together, bare module cost becomes $145,079

Furnace:

$$C_B = \exp\{0.32325 + 0.766[ln(Q)]\}$$

$$F_P = 0.986 - 0.035\left(\frac{\mathrm{P}}{500}\right) + 0.0175\left(\frac{\mathrm{P}}{500}\right)^2$$

$$C_{BM} = F_{BM}F_P\,F_M\,C_B$$

C_{BM} = Bare module cost
C_B = Base cost
P = Operating Pressure (psi)
Q = Heat duty (BTU)
F_P = Pressure factor
F_{BM} = Bare module factor
F_M = Material factor

A.3 Utility Cost Calculation

Power consumption of blower and jet ejector

$$P_B = 0.00436\left(\frac{\mathrm{k}}{\mathrm{k}-1}\right)\left(\frac{Q_I P_I}{\eta_B}\right)\left[\left(\frac{P_O}{P_I}\right)^{\frac{k-1}{k}} - 1\right]$$

$$P_C = \frac{P_B}{\eta_M}$$

P_B = Break horse power (hp)
P_C = Power consumption (hp)
k = specific heat ratio
η_B = Mechanical efficiency
η_M = Motor efficiency
Q_I = Inlet volumetric flow rate (ft^3/min)
P_I = Inlet pressure (psi)
P_O = Outlet pressure (psi)

For inlet blower,

$$P_C = 0.00436\left(\frac{1.4}{1.4-1}\right)\left(\frac{5609.7 * 14.70}{0.75 * 0.9}\right)\left[\left(\frac{23.51}{14.70}\right)^{\frac{1.4-1}{1.4}} - 1\right] = 270.7 \text{ hp}$$

For the vacuum,

$$P_C = 0.00436\left(\frac{1.394}{1.394-1}\right)\left(\frac{4933.5 * 2.205}{0.8 * 0.625}\right)\left[\left(\frac{14.7}{2.205}\right)^{\frac{1.394-1}{1.394}} - 1\right] = 238.1 \text{ hp}$$

Cost of electricity per ton of oxygen,

$$\frac{\text{Cost}}{\text{ton O2}} = (270.7 + 238.1 \text{ hp})\left(\frac{0.746\text{kw}}{\text{hp}}\right)\left(\frac{0.077\$}{\text{kwh}}\right)\left(\frac{24\text{hr}}{\text{day}}\right)\left(\frac{\text{day}}{30\text{tonO2}}\right) = \frac{23.4\$}{\text{ton O2}}$$

Cost of natural gas per ton of oxygen,

$$\left(\frac{4 * 10^{-6}\$}{\text{BTU}}\right)\left(\frac{532216\text{BTU}}{\text{hr}}\right)\left(\frac{24\text{hr}}{\text{day}}\right)\left(\frac{\text{day}}{30\text{tonO2}}\right) = \frac{\$1.70}{\text{ton O2}}$$

Adding the two cost together, the utility cost is 25.1$/ton O2

Appendix B : Heating Cost

Table B.1: Equations used to estimate the cost of the furnace

$T_m = 0.233T_{O2HX}+0.767T$	(eqn. B.1)
$Q = Mc_p(T^*- T_m)$	(eqn. B.2)
$C_B = \exp\{[0.32325+0.76[\ln(Q)]\}$	(eqn. B.3)
$F_p = 0.986-0.0035(P/500)+0.0175(P/500)^2$	(eqn. B.4)
$C_P = F_P F_M C_B$	(eqn. B.5)
$C= C_P F_{BM}$	(eqn. B.6)

Table B.2: Variables used to estimate cost of the furnace

Variable	Unit	Definition
T_{O2HX}	units	Temperature of the outlet stream of the oxygen heat exchanger
T	℃	Temperature of the outlet stream of the waste gas heat exchanger
T_m	℃	Temperature of the inlet stream to the furnace
T*	℃	Inlet temperature to the adsorption chamber
Q	BTU/hr	Heat duty
M	lb/hr	Mass flowrate of air
c_p	BTU/(lb∗℃)	Heat capacity of air, 0.433
C_P	$	f.o.b purchase cost
C_B	$	Base cost
C	$	Cost of Furnace
F_p	Unitless	Pressure factor
F_M	Unitless	Material factor for stainless steel, 1.7
F_{BM}	Unitless	Bare module factor for field-fabricated furnaces, 1.86
P	psig	Pressure of air stream

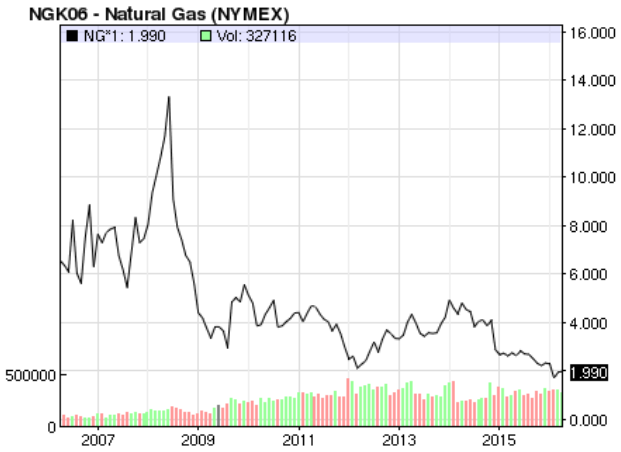

Figure B.1: U.S. National Average Natural Gas Price. This graph was used to estimate the cost of natural gas used in the furnace (Nasdaq, U.S. National Average Natural Gas Price).

Appendix C: ASPEN EDR Files

C.1 Oxygen Heat Exchanger EDR Files

Problem Definition for Oxygen Heat Exchanger

Application Options

Calculation mode	Design (Sizing)
Location of hot fluid	Tube side
Select geometry based on this dimensional standard	SI
Calculation method	Advanced method
Application	Gas, no phase change
Condenser type	Set default
Simulation calculation	Set default
Application	Gas, no phase change
Vaporizer type	Set default
Simulation calculation	Set default
Thermosiphon circuit calculation	Set default

Process Data

		Hot Side		Cold Side	
Fluid name		O2HOT		AIRCO2	
		In	Out	In	Out
Mass flow rate	kg/s	0.3473		0.7316	
Temperature	°C	500	81.92	75.26	
Vapor fraction		1	1	1	1
Pressure	atm	0.2	0.152	1.55	1.502
Pressure at liquid surface in column	bar				
Heat exchanged	kW				
Adjust if over-specified			Heat load		Outlet temperature
Estimated pressure drop	atm		0		0
Allowable pressure drop	kgf/cm^2		0.05		0.05
Fouling resistance	m^2-K/W		0		0

Overall Summary of Oxygen Heat Exchanger

1	Size	447.65	X	3450	mm	Type	BEM	Hor		Connected in	1 parallel	2 series		
2	Surf/Unit (gross/eff/finned)			97.9	/ 96	/			m^2	Shells/unit	2			
3	Surf/Shell (gross/eff/finned)			48.9	/ 48	/			m^2					
4	Design (Sizing)						**PERFORMANCE OF ONE UNIT**							
5				**Shell Side**		**Tube Side**				**Heat Transfer Parameters**				
6	**Process Data**			**In**	**Out**	**In**	**Out**			Total heat load	kW	143.8		
7	Total flow	kg/h		2634		1250				Eff. MTD/ 1 pass MTD	°C	66.91	/	66.6
8	Vapor	kg/h		2634	2634	1250	1250			Actual/Reqd area ratio - fouled/clean		1.01	/	1.01
9	Liquid	kg/s		0	0	0	0							
10	Noncondensable	kg/s		0		0				**Coef./Resist.**	W/(m^2-K)	m^2-K/W		%
11	Cond./Evap.	kg/s		0		0				Overall fouled	22.6	0.04419		
12	Temperature	°C		75.26	268.64	500	81.92			Overall clean	22.6	0.04419		
13	Dew / Bubble point	°C								Tube side film	27.6	0.03628		82.11
14	Quality			1	1	1	1			Tube side fouling		0		0
15	Pressure (abs)	atm		1.55	1.504	0.2	0.157			Tube wall	9811.6	0.0001		0.23
16	DeltaP allow/cal	atm		0.048	0.046	0.048	0.043			Outside fouling		0		0
17	Velocity	m/s		9.46	15.12	74.58	43.55			Outside film	128.2	0.0078		17.66
18	**Liquid Properties**									**Shell Side Pressure Drop**		bar		%
19	Density	kg/m^3								Inlet nozzle		0.00255		5.48
20	Viscosity	mPa-s								InletspaceXflow		0.00534		11.48
21	Specific heat	kJ/(kg-K)								Baffle Xflow		0.01589		34.17
22	Therm. cond.	W/(m-K)								Baffle window		0.0099		21.29
23	Surface tension	N/m								OutletspaceXflow		0.00658		14.15
24	Molecular weight									Outlet nozzle		0.0015		3.22
25	**Vapor Properties**									Intermediate nozzles		0.00473		10.18
26	Density	kg/m^3		1.57	0.98	0.1	0.17			**Tube Side Pressure Drop**		bar		%
27	Viscosity	mPa-s		0.0208	0.0283	0.0415	0.0237			Inlet nozzle		0.00101		2.2
28	Specific heat	kJ/(kg-K)		1.004	1.033	1.048	0.928			Entering tubes		0.00224		4.87
29	Therm. cond.	W/(m-K)		0.0295	0.042	0.0597	0.0309			Inside tubes		0.03349		72.98
30	Molecular weight			28.95	28.95	32	32			Exiting tubes		0.00233		5.08
31	**Two-Phase Properties**									Outlet nozzle		0.00171		3.72
32	Latent heat	kJ/kg								Intermediate nozzles		0.0051		11.12
33	**Heat Transfer Parameters**									**Velocity / Rho*V2**		m/s		$kg/(m-s^2)$
34	Reynolds No. vapor			13605.28	9965.67	2854.88	5005.64			Shell nozzle inlet		14.44		327
35	Reynolds No. liquid									Shell bundle Xflow		9.46	15.12	
36	Prandtl No. vapor			0.71	0.7	0.73	0.71			Shell baffle window		12.88	20.59	
37	Prandtl No. liquid									Shell nozzle outlet		14.68		211
38	**Heat Load**			kW		kW				Shell nozzle interm		15.78		358
39	Vapor only			143.8		-143.8						m/s		$kg/(m-s^2)$
40	2-Phase vapor			0		0				Tube nozzle inlet		47.18		225
41	Latent heat			0		0				Tubes		74.58	43.55	
42	2-Phase liquid			0		0				Tube nozzle outlet		62.29		670
43	Liquid only			0		0				Tube nozzle interm		64.66		696
44	**Tubes**					**Baffles**				**Nozzles: (No./OD)**				
45	Type			Plain		Type	Single segmental					**Shell Side**		**Tube Side**
46	ID/OD	mm	15.75	/ 19.05		Number		4		Inlet	mm	1 / 219.08		1 / 323.85
47	Length act/eff	mm	3450	/ 3383		Cut(%d)	40.79			Outlet		1 / 273.05		1 / 219.08
48	Tube passes		1			Cut orientation		H		Intermediate		1 / 219.08		1 / 219.08
49	Tube No.		237			Spacing: c/c	mm	545		Impingement protection		None		
50	Tube pattern		30			Spacing at inlet	mm	873.98						
51	Tube pitch	mm	23.81			Spacing at outlet	mm	873.98						
52	Insert			None										
53	Vibration problem			Possit / No						RhoV2 violation				No

TEMA Sheet for Oxygen Heat Exchanger

1	Company:								
2	Location:								
3	Service of Unit:		Our Reference:						
4	Item No.:		Your Reference:						
5	Date:	Rev No.:	Job No.:						
6	Size : 448 - 3450 mm	Type: BEM	Horizontal	Connected in: 1 parallel	2 series				
7	Surf/unit(eff.) 96 m^2	Shells/unit 2	Surf/shell(eff.) 48 m^2						
8	**PERFORMANCE OF ONE UNIT**								
9	Fluid allocation			Shell Side		Tube Side			
10	Fluid name			AIRCO2		O2HOT			
11	Fluid quantity, Total		kg/h	2634		1250			
12	Vapor (In/Out)		kg/s	0.7316	0.7316	0.3473	0.3473		
13	Liquid		kg/s	0	0	0	0		
14	Noncondensable		kg/s	0	0	0	0		
15									
16	Temperature (In/Out)		°C	75.26	268.64	500	81.92		
17	Dew / Bubble point		°C						
18	Density Vapor/Liquid		kg/m^3	1.57 /	0.98 /	0.1 /	0.17 /		
19	Viscosity		mPa-s	0.0208 /	0.0283 /	0.0415 /	0.0237 /		
20	Molecular wt, Vap			28.95	28.95	32	32		
21	Molecular wt, NC								
22	Specific heat		kJ/(kg-K)	1.004 /	1.033 /	1.048 /	0.928 /		
23	Thermal conductivity		W/(m-K)	0.0295 /	0.042 /	0.0597 /	0.0309 /		
24	Latent heat		kJ/kg						
25	Pressure (abs)		atm	1.55	1.504	0.2	0.157		
26	Velocity (Mean/Max)		m/s	9.97 / 20.59		54.99 / 74.58			
27	Pressure drop, allow./calc.		atm	0.048	0.046	0.048	0.043		
28	Fouling resistance (min)		m^2-K/W	0		0	0 Ao based		
29	Heat exchanged 143.8	kW			MTD (corrected) 66.91	°C			
30	Transfer rate, Service 22.4		Dirty 22.6		Clean 22.6	W/(m^2-K)			
31	**CONSTRUCTION OF ONE SHELL**					**Sketch**			
32			Shell Side		Tube Side				
33	Design/Vacuum/test pressure	bar	3 / /		3 / /				
34	Design temperature	°C	535		535				
35	Number passes per shell		1		1				
36	Corrosion allowance	mm	0		0				
37	Connections	In mm	1 203.2 / -		1 304.8 / -				
38	Size/Rating	Out	1 254 / -		1 203.2 / -				
39	Nominal	Intermediate	1 203.2 / -		1 203.2 / -				
40	Tube No. 237 OD 19.05 Tks Average 1.65		mm Length 3450		mm Pitch 23.81	mm			
41	Tube type Plain		#/m Material SS 316		Tube pattern 30				
42	Shell SS 316 ID 447.65 OD 457.2		mm	Shell cover -					
43	Channel or bonnet SS 316			Channel cover -					
44	Tubesheet-stationary SS 316 -			Tubesheet-floating -					
45	Floating head cover -			Impingement protection None					
46	Baffle-cross SS 316 Type Single segmental		Cut(%d) 40.79	H Spacing: c/c 545	mm				
47	Baffle-long - Seal Type			Inlet 873.98	mm				
48	Supports-tube U-bend 0			Type					
49	Bypass seal		Tube-tubesheet joint Expanded only (2 grooves)(App.A 'i')						
50	Expansion joint -		Type None						
51	RhoV2-Inlet nozzle 327	Bundle entrance 42		Bundle exit 68	kg/(m-s^2)				
52	Gaskets - Shell side -	Tube side		Flat Metal Jacket Fibe					
53	Floating head -								
54	Code requirements ASME Code Sec VIII Div 1		TEMA class R - refinery service						
55	Weight/Shell 1189 Filled with water 1810.9		Bundle 695.7 kg						
56	Remarks								
57									
58									

C.2 Waste Gas Heat Exchanger EDR Files

Problem Definition for Waste Gas Heat Exchanger

Application Options

Calculation mode	Design (Sizing)
Location of hot fluid	Tube side
Select geometry based on this dimensional standard	SI
Calculation method	Advanced method
Application	Program
Condenser type	Set default
Simulation calculation	Set default
Application	Gas, no phase change
Vaporizer type	Set default
Simulation calculation	Set default
Thermosiphon circuit calculation	Set default

Process Data

		Hot Side		Cold Side	
Fluid name		N2HOT		AIRCN2	
		In	Out	In	Out
Mass flow rate	kg/h	8676		8676	
Temperature	°C	500		75.26	440
Vapor fraction		1		1	1
Pressure	atm	1.2	1	1.5	1.452
Pressure at liquid surface in column	atm				
Heat exchanged	kW				
Adjust if over-specified		Outlet temperature		Heat load	
Estimated pressure drop	atm	0		0	
Allowable pressure drop	atm	0.2		0.048	
Fouling resistance	m^2-K/W	0		0	

Overall Summary of Waste Gas Heat Exchanger

1	Size	598.53	X	5700	mm	Type	BEM	Hor		Connected in	3	parallel	1	series
2	Surf/Unit (gross/eff/finned)			491.2	/ 484.6 /				m^2	Shells/unit	3			
3	Surf/Shell (gross/eff/finned)			163.7	/ 161.5 /				m^2					
4	Design (Sizing)						**PERFORMANCE OF ONE UNIT**							
5					**Shell Side**		**Tube Side**			**Heat Transfer Parameters**				
6	**Process Data**				**In**	**Out**	**In**	**Out**		Total heat load	kW		908.6	
7	Total flow	kg/h			8676		8676			Eff. MTD/ 1 pass MTD	°C	66.81	/	66.79
8	Vapor	kg/h			8676	8676	8676	8676		Actual/Reqd area ratio - fouled/clean		1	/	1
9	Liquid	kg/s			0	0	0	0						
10	Noncondensable	kg/s			0		0			**Coef./Resist.**	W/(m^2-K)	m^2-K/W		%
11	Cond./Evap.	kg/s			0		0			Overall fouled	28.1	0.03556		
12	Temperature	°C			75.26	440	500	149.78		Overall clean	28.1	0.03556		
13	Dew / Bubble point	°C								Tube side film	35.9	0.02785		78.33
14	Quality				1	1	1	1		Tube side fouling		0		0
15	Pressure (abs)	atm			1.5	1.454	1.2	1.169		Tube wall	10103.1	0.0001		0.28
16	DeltaP allow/cal	atm			0.048	0.046	0.2	0.031		Outside fouling		0		0
17	Velocity	m/s			7.53	15.85	16.22	9.1		Outside film	131.5	0.00761		21.39
18	**Liquid Properties**									**Shell Side Pressure Drop**		bar		%
19	Density	kg/m^3								Inlet nozzle		0.00331		7.22
20	Viscosity	mPa-s								InletspaceXflow		0.00292		6.35
21	Specific heat	kJ/(kg-K)								Baffle Xflow		0.02299		50.11
22	Therm. cond.	W/(m-K)								Baffle window		0.00806		17.57
23	Surface tension	N/m								OutletspaceXflow		0.00609		13.27
24	Molecular weight									Outlet nozzle		0.00251		5.48
25	**Vapor Properties**									Intermediate nozzles				
26	Density	kg/m^3			1.52	0.72	0.53	0.94		**Tube Side Pressure Drop**		bar		%
27	Viscosity	mPa-s			0.0208	0.0339	0.035	0.023		Inlet nozzle		0.01832		58.04
28	Specific heat	kJ/(kg-K)			1.004	1.074	1.115	1.046		Entering tubes		0.00035		1.09
29	Therm. cond.	W/(m-K)			0.0295	0.0521	0.0551	0.034		Inside tubes		0.00786		24.91
30	Molecular weight				28.95	28.95	28.01	28.01		Exiting tubes		0.00028		0.88
31	**Two-Phase Properties**									Outlet nozzle		0.00476		15.08
32	Latent heat	kJ/kg								Intermediate nozzles				
33	**Heat Transfer Parameters**									**Velocity / Rho*V2**		m/s		kg/(m-s^2)
34	Reynolds No. vapor				10483.35	6418.8	3871.06	5894.45		Shell nozzle inlet		16.39		408
35	Reynolds No. liquid									Shell bundle Xflow		7.53	15.85	
36	Prandtl No. vapor				0.71	0.7	0.71	0.71		Shell baffle window		9.53	20.05	
37	Prandtl No. liquid									Shell nozzle outlet		21.95		347
38	**Heat Load**					kW		kW		Shell nozzle interm				
39	Vapor only					908.6		-908.6				m/s		kg/(m-s^2)
40	2-Phase vapor					0		0		Tube nozzle inlet		81.34		3506
41	Latent heat					0		0		Tubes		16.22	9.1	
42	2-Phase liquid					0		0		Tube nozzle outlet		45.71		1970
43	Liquid only					0		0		Tube nozzle interm				
44	**Tubes**						**Baffles**			**Nozzles: (No./OD)**				
45	Type					Plain	Type	Single segmental				**Shell Side**		**Tube Side**
46	ID/OD		mm	15.75	/	19.05	Number		8	Inlet	mm	1 / 219.08	1	/ 168.28
47	Length act/eff		mm	5700	/	5623	Cut(%d)		39.66	Outlet		1 / 273.05	1	/ 168.28
48	Tube passes			1			Cut orientation		H	Intermediate		/		/
49	Tube No.			480			Spacing: c/c	mm	590	Impingement protection		None		
50	Tube pattern			30			Spacing at inlet	mm	746.48					
51	Tube pitch		mm	23.81			Spacing at outlet	mm	746.48					
52	Insert					None								
53	Vibration problem				Possit	/ No				RhoV2 violation				No

TEMA Sheet for Waste Gas Heat Exchanger

1	Company:							
2	Location:							
3	Service of Unit:		Our Reference:					
4	Item No.:		Your Reference:					
5	Date:	Rev No.:	Job No.:					
6	Size : 599 - 5700 mm	Type: BEM	Horizontal		Connected in: 3 parallel	1 series		
7	Surf/unit(eff.) 484.6 m^2	Shells/unit 3			Surf/shell(eff.)	161.5 m^2		
8	**PERFORMANCE OF ONE UNIT**							
9	Fluid allocation		Shell Side		Tube Side			
10	Fluid name		AIRCN2		N2HOT			
11	Fluid quantity, Total	kg/h	8676		8676			
12	Vapor (In/Out)	kg/s	2.41	2.41	2.41	2.41		
13	Liquid	kg/s	0	0	0	0		
14	Noncondensable	kg/s	0	0	0	0		
15								
16	Temperature (In/Out)	°C	75.26	440	500	149.78		
17	Dew / Bubble point	°C						
18	Density Vapor/Liquid	kg/m^3	1.52 /	0.72 /	0.53 /	0.94 /		
19	Viscosity	mPa-s	0.0208 /	0.0339 /	0.035 /	0.023 /		
20	Molecular wt, Vap		28.95	28.95	28.01	28.01		
21	Molecular wt, NC							
22	Specific heat	kJ/(kg-K)	1.004 /	1.074 /	1.115 /	1.046 /		
23	Thermal conductivity	W/(m-K)	0.0295 /	0.0521 /	0.0551 /	0.034 /		
24	Latent heat	kJ/kg						
25	Pressure (abs)	atm	1.5	1.454	1.2	1.169		
26	Velocity (Mean/Max)	m/s	10.46 / 20.05		11.66 / 16.22			
27	Pressure drop, allow./calc.	atm	0.048	0.046	0.2	0.031		
28	Fouling resistance (min)	m^2-K/W	0		0	0 Ao based		
29	Heat exchanged 908.6	kW			MTD (corrected)	66.81 °C		
30	Transfer rate, Service 28.1		Dirty 28.1		Clean 28.1		W/(m^2-K)	
31	**CONSTRUCTION OF ONE SHELL**						**Sketch**	
32			Shell Side		Tube Side			
33	Design/Vacuum/test pressure	bar	3 /	/	3 /	/		
34	Design temperature	°C	475		535			
35	Number passes per shell		1		1			
36	Corrosion allowance	mm	0		0			
37	Connections	In mm	1 203.2 /	-	1 152.4 /	-		
38	Size/Rating	Out	1 254 /	-	1 152.4 /	-		
39	Nominal	Intermediate	/	-	/	-		
40	Tube No. 480 OD 19.05 Tks Average 1.65		mm Length 5700		mm Pitch 23.81	mm		
41	Tube type Plain		#/m Material SS 316		Tube pattern 30			
42	Shell SS 316 ID 598.53 OD 609.6	mm	Shell cover -					
43	Channel or bonnet SS 316		Channel cover -					
44	Tubesheet-stationary SS 316 -		Tubesheet-floating -					
45	Floating head cover -		Impingement protection None					
46	Baffle-cross SS 316	Type Single segmental	Cut(%d) 39.66	H Spacing: c/c 590	mm			
47	Baffle-long -	Seal Type	Inlet 746.48	mm				
48	Supports-tube U-bend	0	Type					
49	Bypass seal	Tube-tubesheet joint	Expanded only (2 grooves)(App.A 'i')					
50	Expansion joint -	Type None						
51	RhoV2-Inlet nozzle 408	Bundle entrance 104	Bundle exit 219	kg/(m-s^2)				
52	Gaskets - Shell side -	Tube side	Flat Metal Jacket Fibe					
53	Floating head -							
54	Code requirements ASME Code Sec VIII Div 1		TEMA class R - refinery service					
55	Weight/Shell 2995.6 Filled with water 4508.8		Bundle 2190.5 kg					
56	Remarks							
57								
58								

Appendix D: Solar Salt Properties

Composition: 60% $NaNO_3$, 40 % KNO_3
Temperature Range: 220-600℃
Heat Capacity @ 300 C: 1495 J/kg-K
Density: 1899 kg/m^3
Cost: 0.49 $/kg

Appendix E : Operating Cost Sensitivity Analysis

Adsorber inlet temperature (℃)	Adsorber inlet pressure (atm)	Adsorber inlet air flow velocity (m/s)	MIEC cost($/tonO2)	Adsorber cost($/tonO2)	Blower+ejector cost($/tonO2)	Heat exchangers + Furnace cost($/tonO2)	Total production cost ($tonO2)
300	1.25	0.03	$114.76	$33.73	$23.59	$5.75	$177.83
300	1.25	0.10	$37.73	$12.66	$23.92	$5.75	$80.07
300	1.25	0.32	$12.74	$5.31	$24.51	$5.75	$48.31
300	1.25	1.00	$4.03	$2.41	$24.50	$5.75	$36.68
300	1.25	3.16	$0.78	$1.07	$20.90	$5.75	$28.50
300	1.25	10.00	$0.94	$1.15	$36.82	$5.75	$44.66
300	1.5	0.03	$91.13	$27.29	$27.98	$5.08	$151.49
300	1.5	0.10	$30.68	$10.68	$28.80	$5.08	$75.25
300	1.5	0.32	$10.30	$4.54	$29.63	$5.08	$49.56
300	1.5	1.00	$3.19	$2.10	$29.35	$5.08	$39.72
300	1.5	3.16	$1.33	$1.36	$33.82	$5.08	$41.60
300	1.5	10.00	$0.72	$1.02	$46.92	$5.08	$53.74
300	2	0.03	$68.33	$21.20	$36.08	$3.76	$129.37
300	2	0.10	$23.57	$8.58	$37.95	$3.76	$73.87
300	2	0.32	$7.75	$3.71	$38.84	$3.76	$54.05
300	2	1.00	$2.53	$1.87	$39.57	$3.76	$47.73
300	2	3.16	$1.11	$1.23	$48.97	$3.76	$55.06
300	2	10.00	$0.72	$1.02	$84.12	$3.76	$89.62
300	3	0.03	$46.95	$15.26	$49.77	$3.31	$115.30
300	3	0.10	$16.24	$6.43	$52.99	$3.31	$78.97
300	3	0.32	$4.91	$2.73	$51.37	$3.31	$62.33
300	3	1.00	$1.69	$1.52	$54.59	$3.31	$61.12
300	3	3.16	$0.89	$1.14	$80.22	$3.31	$85.56
300	3	10.00	$0.50	$0.89	$130.24	$3.31	$134.94
500	1.25	0.03	$154.60	$44.35	$23.58	$8.63	$231.17
500	1.25	0.10	$50.51	$16.20	$23.86	$8.63	$99.19

500	1.25	0.32	$17.10	$6.66	$24.46	$8.63	$56.86
500	1.25	1.00	$5.25	$2.85	$24.19	$8.63	$40.92
500	1.25	3.16	$2.17	$1.71	$26.90	$8.63	$39.41
500	1.25	10.00	$1.17	$1.28	$35.02	$8.63	$46.10
500	1.5	0.03	$124.89	$36.38	$28.18	$7.69	$197.15
500	1.5	0.10	$41.26	$13.66	$28.76	$7.69	$91.37
500	1.5	0.32	$13.88	$5.66	$29.62	$7.69	$56.84
500	1.5	1.00	$4.44	$2.59	$29.79	$7.69	$44.51
500	1.5	3.16	$1.64	$1.47	$32.18	$5.23	$40.51
500	1.5	10.00	$0.89	$1.14	$44.16	$5.23	$51.42
500	2	0.03	$93.16	$27.90	$36.30	$5.80	$163.16
500	2	0.10	$31.60	$10.94	$37.81	$5.80	$86.15
500	2	0.32	$10.44	$4.57	$38.82	$5.80	$59.63
500	2	1.00	$3.39	$2.19	$39.42	$5.80	$50.80
500	2	3.16	$1.39	$1.37	$46.51	$5.80	$55.08
500	2	10.00	$0.89	$1.14	$78.14	$5.80	$85.97
500	3	0.03	$63.14	$19.72	$49.67	$6.72	$139.25
500	3	0.10	$21.80	$8.03	$52.79	$6.72	$89.34
500	3	0.32	$6.58	$3.32	$51.11	$6.72	$67.73
500	3	1.00	$2.36	$1.79	$55.87	$6.72	$66.75
500	3	3.16	$1.11	$1.23	$75.50	$6.72	$84.56
500	3	10.00	$0.61	$0.95	$119.55	$6.72	$127.84
700	1.25	0.03	$192.67	$54.39	$23.50	$11.74	$282.31
700	1.25	0.10	$64.03	$19.98	$23.92	$11.74	$119.68
700	1.25	0.32	$21.63	$8.00	$24.51	$11.74	$65.88
700	1.25	1.00	$6.89	$3.43	$24.57	$11.74	$46.63
700	1.25	3.16	$2.53	$1.87	$26.05	$11.74	$42.20
700	1.25	10.00	$1.53	$1.45	$35.81	$11.74	$50.53
700	1.5	0.03	$156.85	$44.90	$28.15	$10.53	$240.44
700	1.5	0.10	$52.06	$16.68	$28.79	$10.53	$108.06

700	1.5	0.32	$17.41	$6.79	$29.56	$10.53	$64.29
700	1.5	1.00	$5.50	$2.95	$29.54	$10.53	$48.52
700	1.5	3.16	$2.17	$1.71	$33.03	$10.53	$47.43
700	1.5	10.00	$1.17	$1.28	$45.39	$10.53	$58.37
700	2	0.03	$117.87	$34.56	$36.41	$8.10	$196.94
700	2	0.10	$39.96	$13.34	$37.92	$8.10	$99.31
700	2	0.32	$13.16	$5.46	$38.85	$8.10	$65.57
700	2	1.00	$4.14	$2.48	$38.71	$8.10	$53.43
700	2	3.16	$1.80	$1.54	$47.53	$8.10	$58.98
700	2	10.00	$1.17	$1.28	$80.80	$8.10	$91.35
700	3	0.03	$80.02	$24.33	$49.90	$9.96	$164.22
700	3	0.10	$27.49	$9.69	$52.87	$9.96	$100.01
700	3	0.32	$8.30	$3.93	$51.19	$9.96	$73.39
700	3	1.00	$3.11	$2.08	$57.76	$9.96	$72.92
700	3	3.16	$1.47	$1.39	$78.64	$9.96	$91.47
700	3	10.00	$0.81	$1.08	$124.44	$9.96	$136.29

Appendix F : Break even point Analysis

F.2 Increased Selling Price of Oxygen

The Internal Rate of Return (IRR) for this project is		-3.25%
The Net Present Value (NPV) of this project in 2016 is	$	(736,900)

ROI Analysis (Third Production Year)

Annual Sales	**526,061**
Annual Costs	**(436,057)**
Depreciation	**(90,086)**
Income Tax	**30**
Net Earnings	**(52)**
Total Capital Investment	**1,183,319**
ROI	**0.00%**

Figure F.1.1 : Profitability Analysis

F.2 Tuned Kinetic Constant and Loading Capacity

The Internal Rate of Return (IRR) for this project is -3.00%

The Net Present Value (NPV) of this project in 2016 is $ (531,500)

ROI Analysis (Third Production Year)

Annual Sales	**370,799**
Annual Costs	**(302,946)**
Depreciation	**(65,573)**
Income Tax	**(844)**
Net Earnings	**1,436**
Total Capital Investment	**860,242**
ROI	**0.17%**

Figure F.2.1 : Profitability Analysis

Table F.2.1 : Utility Costs per ton of oxygen

Utility	Unit	Required energy per ton O2	Cost per Unit [$/kwh]	Cost/ton O2 [$/ton]
Electricity	kWh	197	0.077	15.2
Natural Gas	kWh	121	0.014	1.70
			Total Utilities Cost	16.9

Table F.2.2: Equipment Bare Module Cost

Equipment	Type	Bare-module cost
Centrifugal Blower	Process Machinery	$50,600
Jet Ejector	Process Machinery	$13,400
Furnace	Fabricated Equipment	$104,800
Adsorption Chamber	Fabricated Equipment	$76,900
Heat Exchanger 1	Fabricated Equipment	$177,800
Heat Exchanger 2	Fabricated Equipment	$64,700
MIEC Sorbents	Compound in System	$72,600
Solar Salt	Compound in System	$600
Total bare module cost:		$561,400

Variable Costs at 100% Capacity:

General Expenses

Selling / Transfer Expenses:		$	11,880
Direct Research:		$	19,008
Allocated Research:		$	1,980
Administrative Expense:		$	7,920
Management Incentive Compensation:		$	4,950
Total General Expenses		$	45,738
Raw Materials	$0.000000 per tons of O2		$0
Byproducts	$0.000000 per tons of O2		$0
Utilities	$16.863000 per tons of O2		$166,944
Total Variable Costs		**$**	**212,682**

Figure F.2.2 : Annual Variable Costs

Operations		
Direct Wages and Benefits	$	-
Direct Salaries and Benefits	$	-
Operating Supplies and Services	$	-
Technical Assistance to Manufacturing	$	-
Control Laboratory	$	-
Total Operations	**$**	**-**
Maintenance		
Wages and Benefits	$	32,933
Salaries and Benefits	$	8,233
Materials and Services	$	32,933
Maintenance Overhead	$	1,647
Total Maintenance	**$**	**75,746**
Operating Overhead		
General Plant Overhead:	$	2,923
Mechanical Department Services:	$	988
Employee Relations Department:	$	2,429
Business Services:	$	3,046
Total Operating Overhead	**$**	**9,386**
Property Taxes and Insurance		
Property Taxes and Insurance:	$	14,637
Other Annual Expenses		
Rental Fees (Office and Laboratory Space):	$	-
Licensing Fees:	$	-
Miscellaneous:	$	-
Total Other Annual Expenses	**$**	**-**
Total Fixed Costs	**$**	**99,768**

Figure F.2.3: Fixed Costs Summary

Total Bare Module Costs:			
Fabricated Equipment	$	440,099	
Process Machinery	$	50,574	
Spares	$	-	
Storage	$	-	
Other Equipment	$	73,149	
Catalysts	$	-	
Computers, Software, Etc.	$	-	
Total Bare Module Costs:			**$ 563,823**
Direct Permanent Investment			
Cost of Site Preparations:	$	28,191	
Cost of Service Facilities:	$	28,191	
Allocated Costs for utility plants and related facilities:	$	-	
Direct Permanent Investment			**$ 620,205**
Total Depreciable Capital			
Cost of Contingencies & Contractor Fees	$	111,637	
Total Depreciable Capital			**$ 731,842**
Total Permanent Investment			
Cost of Land:	$	14,637	
Cost of Royalties:	$	-	
Cost of Plant Start-Up:	$	73,184	
Total Permanent Investment - Unadjusted			$ 819,663
Site Factor			1.00
Total Permanent Investment			**$ 819,663**

Figure F.2.4 : Investment Summary

	2019	2020	2021
Accounts Receivable	$ 14,647	$ 7,323	$ 7,323
Cash Reserves	$ 9,865	$ 4,932	$ 4,932
Accounts Payable	$ (6,175)	$ (3,087)	$ (3,087)
O2 Inventory	$ 1,953	$ 976	$ 976
Raw Materials	$ -	$ -	$ -
Total	**$ 20,290**	**$ 10,145**	**$ 10,145**
Present Value at 15%	*$ 13,341*	*$ 5,800*	*$ 5,044*

Total Capital Investment **$ 843,848**

Figure F.2.5 : Working Capital Summary

Appendix G : Selected Images Illustrating the Use of COMSOL

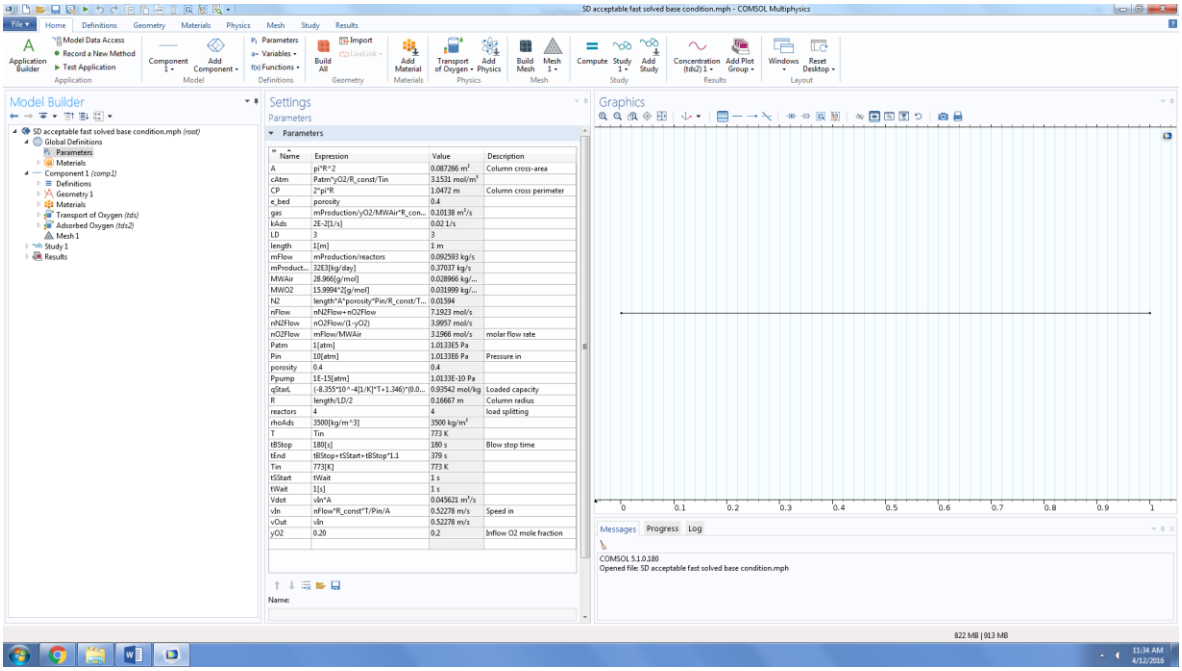

Figure G.5.1: Parameter list in COMSOL with 1-D adsorption chamber modeled on right.

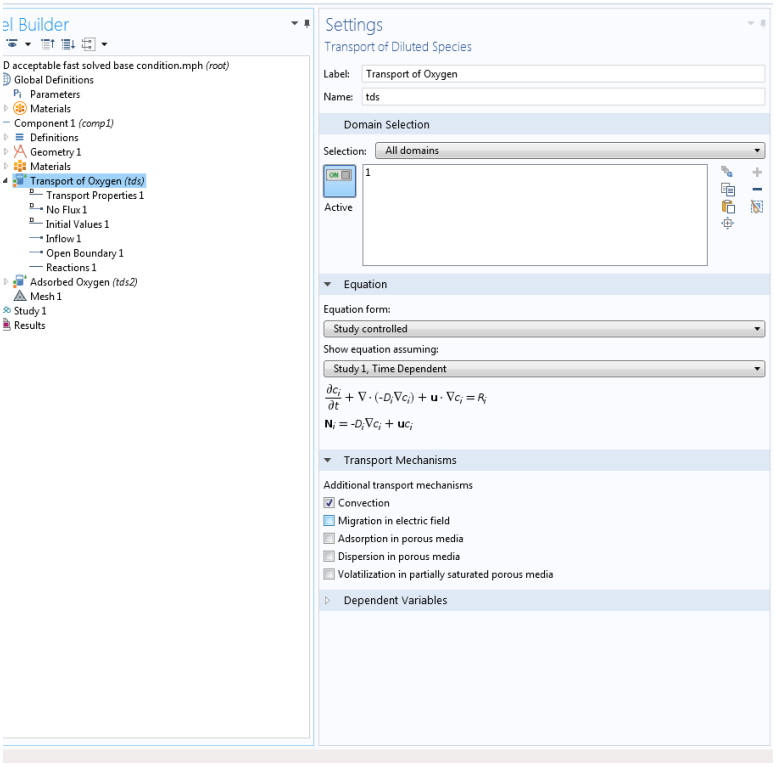

Figure G.5.2: Selection and entry of equation parameters in COMSOL.

Figure G.5.3: Point distribution in mesh used to simulate adsorption chamber behavior.

Appendix H: Standard Operating Procedure

DANGER:
IMPROPER OPERATION OF PLANT CONTROLS MAY RESULT IN ELECTRICAL SHOCK, SERIOUS INJURY, OR EVEN DEATH. DO NOT OPERATE PLANT CONTROLS WITHOUT UNDERSTANDING PLANT EQUIPMENT AND TRAINING.

WARNING:
Only technicians with Level 1 safety training should start up the plant.

Plant Startup

1) Ensure valves 1-55 are closed.
2) Turn primary control switch counter-clockwise to AUTO.

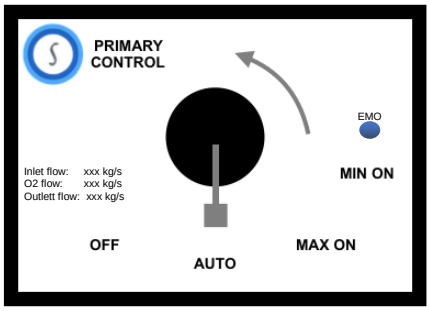

WARNING: Do not switch to “MAX ON” or “MIN ON” unless instructed by a Level 2 technician.

3) Check no leak indications have been triggered.
4) Ensure furnace indicator is GREEN
5) Ensure heat exchanger indicators are GREEN
6) Ensure blower indicator is GREEN
7) Ensure vacuum indicator is GREEN
8) Ensure outlet indicator is GREEN

Check indicated flow rates on control panel in the middle left. Inlet flow rate should be ~2.0 kg/s. O2 flow rate ~0.35 kg/s. Outlet flow rate ~1.65 kg/s